CHALMERS
UNIVERSITY OF TECHNOLOGY

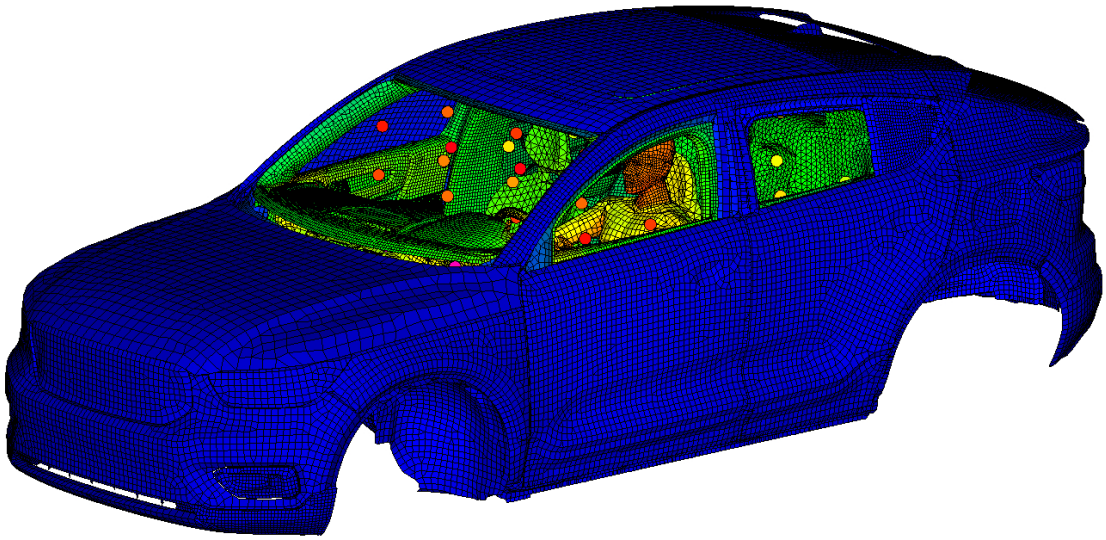

Energy efficient heating for cabin climate comfort

Using localized heating

Master's thesis in Mobility Engineering

MARCEL DANILUK

DEPARTMENT OF MECHANICS AND MARITIME SCIENCES

CHALMERS UNIVERSITY OF TECHNOLOGY
Gothenburg, Sweden 2024
www.chalmers.se

Master's thesis 2024

Energy efficient heating for cabin climate comfort

Using localized heating

MARCEL DANILUK

CHALMERS
UNIVERSITY OF TECHNOLOGY

Department of Mechanics and Maritime Sciences
Division of Fluid Dynamics
Chalmers University of Technology
Gothenburg, Sweden 2024

Energy efficient heating for cabin climate comfort
Using localized heating
MARCEL DANILUK

Supervisor: Martin Svensson, Volvo Cars
Examiner: Håkan Nilsson, Department of Mechanics and Maritime Sciences, Division of Fluid Dynamics, Chalmers University of Technology

Master's Thesis 2024
Department of Mechanics and Maritime Sciences
Division of Fluid Dynamics
Chalmers University of Technology
SE-412 96 Gothenburg
Telephone +46 31 772 1000

Cover: Image of a car cabin thermal simulation in TAITherm showing temperature of the surfaces.

Typeset in LaTeX
Gothenburg, Sweden 2024

Energy efficient heating for cabin climate comfort
Using localized heating
MARCEL DANILUK,
Department of Mechanics and Maritime Sciences
Chalmers University of Technology

Abstract

In recent years, the automotive sector has experienced a notable upsurge in the popularity of electric vehicles (EVs), as evidenced by the expanding array of EV models introduced to the market. This trend reflects a significant transition towards sustainable transportation solutions, promising reduced carbon emissions and decreased reliance on fossil fuels. However, alongside the promising prospects associated with the rise of EVs, there are notable challenges that must be addressed to facilitate their widespread adoption. A primary challenge confronting the adoption of electric vehicles pertains to battery technology. The current capacity and efficiency of batteries remain focal points for improvement. The constraints imposed by battery capacity directly influence the driving range of EVs, therefore impacting consumer confidence and adoption rates. Moreover, adverse weather conditions, particularly in cold climates, exacerbate these limitations by imposing additional strain on battery performance. The heating, ventilation, and air conditioning (HVAC) system is a significant contributor to energy consumption in EVs. In cold climates, the energy-intensive process of cabin heating assumes paramount importance, given its potential to significantly diminish the vehicle's range.
This thesis investigates radiation panels as an alternative approach to the heating of the cabin, alongside traditional heating done with warm air from the HVAC system and conductive heating from the seat and the steering wheel. A numerical model was developed in TAITherm software that simulates the heat up sequence of a cabin of an SUV-type car in -7$°C$ outside temperature. The model includes a driver manikin with a human thermal model, which calculates the human's perceived sensation and comfort. A parameter space was defined for the simulations and a comparison between the cases was made.

Keywords: local heating, electric vehicle, human comfort, cabin heat up, energy efficiency.

Acknowledgements

This thesis is a part of Masters in Mobility Engineering at Chalmers University of Technology. The work was carried out at Volvo Cars Corporation with the help of supervisor Martin Svensson, and an examiner at Chalmers, Prof. Håkan Nilsson.

I would like to thank everyone at the climate department at Volvo for the help and resources provided. I want to thank my supervisor Martin Svensson especially for creating this thesis opportunity. His constant support, optimism, and patience were invaluable during this work. Additionally, I would like to thank Kameswara Kethireddy and the support staff at ThermoAnalytics for providing me with necessary licenses and their help with the software. Lastly, I acknowledge Prof. Håkan Nilsson from Chalmers University of Technology for guidance during the master's program and for being my examiner.

Marcel Daniluk, Gothenburg, May 2024

List of Acronyms

Below is the list of acronyms that have been used throughout this thesis listed in alphabetical order:

AC	Air Conditioning
BEV	Battery-powered Electric Vehicle
CFD	Computational Fluid Dynamics
EU	European Union
EV	Electric Vehicle
HVAC	Heating Ventilation and Air Conditioning
ICE	Internal Combustion Engine
SUV	Sport Utility Vehicle
TTC	Time to Comfort
VCC	Volvo Cars Corporation

Contents

List of Figures

List of Tables

1
Introduction

1.1 Background

Due to environmental and sustainability concerns more and more new cars are electric. The transition to EVs is driven by a myriad of reasons. These include (among others):

- political influences, such as EU's regulations on vehicle emissions (EURO 6, EURO 7)
- social pressure to limit the use of fossil fuels and air pollution in cities
- environmental concerns, climate change and global warming due to emissions

While EVs have a lot of benefits compared to the ICE cars they come with their own challenges. One of the main issues of the current era BEVs is the limited capacity of the batteries which translates to a short range of the car. In order to extend the range both academia and industry is researching ways to optimize the energy usage in the vehicle.

One of the systems which drains the battery energy is the climate control of the passenger cabin. The topic of climate control in a vehicle cabin is covered well in many publications. Basics of climate control are covered extensively in G.D. Mathur's book [1].

1.2 Previous studies

Substantial research has been carried out to optimize the cooling and AC, which is the most often used function of the HVAC system in hotter climates. However, in colder climates heating can have a noticeable impact on the energy usage of the vehicle, and historically it has often been neglected due to the abundant waste heat from ICE in older cars. Newer, more optimized engines have lower losses and therefore less waste heat is available, but this has been solved by using for example fuel operated heaters (FOH). Energy efficiency of cabin climate in ICE based cars has been thoroughly investigated in the Ph.D. thesis by F. Nielsen [2] done at Chalmers in collaboration with Volvo Cars. Since no fuel is immediately available to burn in case of a BEV, other solutions need to be developed in order to achieve energy efficient heating. Most current designs of EVs heat up the air in the ventilation system, a method adapted from ICE cars. Is there another way to achieve thermal

comfort of the passengers in cold outside conditions that is more suited for use in EVs? Can it be done whilst also reducing the energy used?

The problem of range reduction of EVs in cold climate has been acknowledged in the recent years. To quote Jeffers et. al. "When operated, the cabin climate control system is the largest auxiliary load on a vehicle. This load has significant impact on fuel economy for conventional and hybrid vehicles, and it drastically reduces the driving range of all-electric vehicles (EVs)." In this document it is stated that at the outside temperature of -20°F (-6.66°C) it can reduce EV range by 20%-59% [3]. Strategies such as zonal heating was investigated in this paper to reduce the overall energy usage.

Some research was done where alternative heating strategies were investigated. The paper by Wang et. al. introduced a heat pump coupled with an AC unit into the EV. [4] Since heat pumps usually have a low efficiency in low temperature the coupled system tries to overcome that. In this research the target is to reach a set temperature in the cabin (18°C).

Another approach to energy efficiency is limiting the heat loss by improving insulation. In a recent paper Anandh et. al. [5] investigate potential energy saving by comparing change in mean temperature of the baseline and insulated models.

Complex computational studies were performed using human comfort models. [6] The comfort models are an alternative option that can be used instead of a target temperature when analyzing and designing a climate control system. Both approaches ultimately aim to make the driver and passengers thermally comfortable. The first method with the set target temperature assumes that at that temperature the person will be comfortable. This approach is easy to implement in both numerical simulations as well as physical testing. However, it is difficult to estimate effects of heating localized on the person. The human physiology model is capable of capturing the effects of localized heating in a way that would be hard to capture with just the cabin air temperature. The downside of the human physiology and comfort models is that they require significantly more setup in a numerical simulation and additional equipment i.e. a manikin in physical tests.

In the Nielsen's thesis, researching localized heating is recommended as future work. [2]

1.3 Preliminary aim

The purpose of this thesis is to investigate alternative ways in which the cabin heating of an electric car can be achieved while still maintaining climate comfort. Is it possible to lower the energy usage with these different methods? One of the important aspects of climate control is to evaluate the comfort of the passengers. For example, a passenger who feels that the automatic heating system is not doing a good enough work, might manually switch it to maximum, defeating the purpose

of optimizing the heat delivery. Based on that assumption, the investigation should not only focus on the simulation of heating up the cabin, but also consider the way the heat is delivered to the person seating in the seat.

Convectional heating through HVAC is already addressed and well understood. Therefore, radiative and conductive heating elements will be the main points of interest. However, convective heating of the air might still be necessary for defrosting and defogging the windshield hence it still needs to be accounted for. Other solutions should be viable for passenger comfort, such as localized heating. This thesis will study heating elements such as surface heating in various locations in the cabin. The aim of this approach is to use localized heating on the passengers and in the process use less energy than when controlling the climate in the whole cabin through heating of the air, while at the same time providing adequate comfort.

1.4 Objectives

The expected outcome of the project is the numerical analysis of different ways of heating the cabin of the electric car and the resulting comfort. The main objective is to perform multiple simulations, each using different combinations of heating strategies. The results will be compared in order to find the most optimal way to achieve climate comfort with the least amount of energy used. Moreover, the safety concerns should be considered. The systems under investigation are directly connected to human comfort and safety. Therefore, care needs to be taken when evaluating the possible solutions. For example, hypothetically during optimization process it might turn out that one surface heated to a high temperature is more effective than two surfaces with lower temperatures, however this higher temperature is high enough to burn a person who touches it. Hence during the process, the temperature should be bounded by some maximum safety value. In the given example this value is most likely found in related regulation. For cases where no formal regulation exists it would be the designer's responsibility to determine safety limits either based on supplementary material or testing.

2

Theory

Heat transfer is a process of exchanging thermal energy between the elements of the system, the heat flows from a region with higher temperature to a region of lower temperature. The transfer of heat can be divided into three primary mechanisms: conduction, convection and radiation. Here a brief explanation of each is given based on the information from the textbook by F.P. Incropera [15].

2.1 Conduction

Conduction is transfer of heat through a material medium by collisions of neighbouring molecules. It occurs inside the material and between elements in contact with each other. The molecules vibrate about their equilibrium positions and transfer thermal energy to adjacent molecules. Conduction is governed by Fourier's law given by (in 1D)

$$Q_{conduction} = -kA\frac{dT}{dx}, \tag{2.1}$$

where k is the thermal conductivity of the material, A is the cross-sectional area normal to the direction of heat flow, and $\frac{dT}{dx}$ is the temperature gradient along the direction of heat transfer.

2.2 Convection

Convection involves the transfer of heat through the movement of a fluid medium, such as a liquid or gas. This mechanism combines both conduction and advection, as heat is transported by the bulk movement of the fluid molecules. The rate of convective heat transfer at a surface between a solid and a fluid is described by Newton's law of cooling, expressed as

$$Q_{convection} = hA(T_s - T_f), \tag{2.2}$$

where h is the convective heat transfer coefficient, A is the surface area through which heat is transferred, T_s is the surface temperature, and T_f is the freestream temperature of the fluid, at some distance to the surface where it is not directly influenced by the surface.

2.3 Radiation

Radiation is the heat transfer by electromagnetic waves emitted from a surface. All objects emit thermal radiation proportional to their temperature, according to the Stefan-Boltzmann law given by

$$Q_{radiation} = \varepsilon \sigma A T_s^4, \tag{2.3}$$

where ε is the emissivity of the surface between 0 and 1, σ is the Stefan Boltzmann constant equal to $5.67 * 10^{-8}\ Wm^{-2}K^{-4}$, A is the surface area, and T_s is the absolute temperature of the surface.

Unlike conduction and convection, radiation does not require a medium. It means that even if surfaces are separated with a vacuum they can still exchange heat via radiation.

2.4 TAITherm

The computations in this thesis are primarily done in TAITherm software. It is a commercial numerical code for heat transfer simulations. It specializes in radiation and conduction calculation between surfaces of solids. It also calculated convection. It operates on a meshed model where partial differential equations are solved. The TAITherm solver uses the Finite Volume Method in the spatial domain and the Finite Difference Method in the time domain. Each element in the mesh is modeled as two surfaces (front and back) separated by a specified thickness, and each surface has an associated thermal node. Each thermal node is associated with the surface and with one-half of the volume that is bounded by the two surfaces (see Figure 2.1). A single temperature is assumed for the volume that is associated with each thermal node. Elements can be assigned to a Part. All elements withing a single part have the same thermal properties and can be edited in bulk, however, the solution is still performed at the element level.

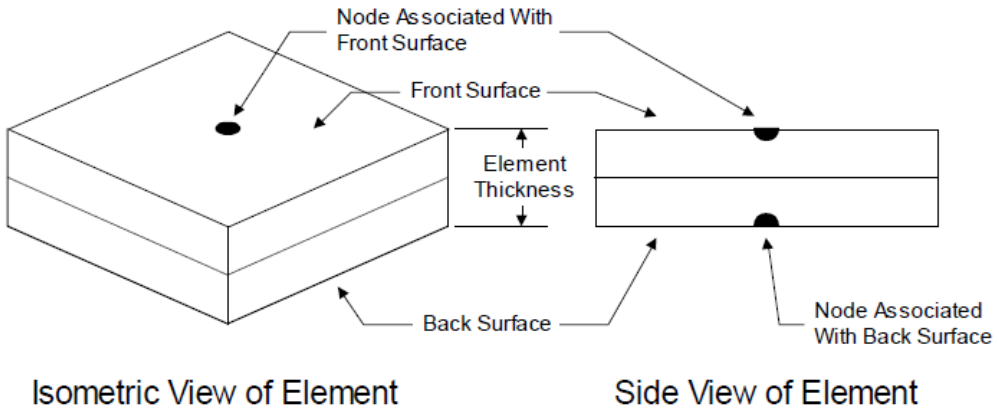

Figure 2.1: Mesh element and associated nodes in TAITherm.

The code calculates the governing equations at every node. The first law of thermodynamics for each node is

$$mC_p\frac{\partial T_k}{\partial t} = Q_{convection} + Q_{conduction} + Q_{radiation} + Q_{imposed}, \tag{2.4}$$

where m is the mass of the node, T is the node temperature, and C_p is the specific heat of the material. Each Q term corresponds to the heat transfer mode described previously and imposed heat is the auxiliary heat that can be imposed by the user for example to model the electrical heat generation.

In TAITherm conduction is calculated using eq. 2.1 between the nodes of elements that share at least one edge with each other. It is possible to also add convection connections between elements that do not share an edge. This feature is called ¨Thermal link¨ and it has two types. Face-to-face thermal links are used to make a connection between parts in close proximity to each other. It creates pairs of elements from each part in view of each other in a specified offset distance. The pairs exchange heat via conduction using thermal conductivity specified for the link. It is useful when connecting two dissimilar meshes such as a human and a seat. The second type are generic links which connect specified elements to each other. It can be used to connect elements faces that are geometrically not sufficiently close to each other or oriented in a way that the face-to-face thermal links are not captured.

If convection is enabled for the given element it is calculated with the previously described formula 2.2. For convection calculations the convective heat transfer is specified for each element. It can be either inserted by the user or calculated using one of many TAITherm built-in libraries. The fluid temperature can be set by the user or the temperature of a fluid part can be used. The fluid part is a one-dimensional part, a single fluid node that represents some volume of fluid for example the air in proximity with the surface. If no volume is specified then the solver will compute a steady state temperature of the part at each time step. Fluid parts can be connected to other fluid parts via advection links which model the transport of heat between regions caused by the movement of the fluid. If the fluid part has a specified position then the surface elements can assign convection to be modeled from geometric parts to the nearest fluid part position.

The radiation between two surfaces is computed using view factors. A view factor basically describes how much of the second surface is in view of the first. When the view factor is included in equation 2.3 the radiative heat transfer from surface 1 to surface 2 becomes

$$Q_{radiation,1\to2} = \frac{\sigma A_1(T_1^4 - T_2^4)}{\frac{1-\varepsilon_1}{\varepsilon_1} + \frac{1}{F_{1\to2}} + \frac{A_1}{A_2} * \frac{1-\varepsilon_2}{\varepsilon_2}}, \tag{2.5}$$

where the symbols are the same as in the equation 2.3 with the subscripts 1 and 2 denoting values of surface 1 and 2 respectively and $F_{1\to2}$ is the view factor from the

first to the second surface. The equation in this form is described in Chapter 5 in [15].

2.5 Human Physiology

Heat transfer to and from the human body is governed by the conduction, convection and radiation equations that were described above. The body consists of materials with different thermal properties such as bone, muscle, fat, skin etc.. Moreover, the human nervous system actively regulates the temperature of the body. It is done by causing sweating, shivering, changes in blood flow by vasoconstriction and vasodilation. In this work a human model is used. The TAITherm human model consists of surface elements with multiple layers representing bone, muscle, fat, skin etc. It includes the aforementioned human thermoregulation processes. The thermoregulation calculations are based on Fiala et. al. [8]. A more detailed description of how the human thermal model is implemented in TAITherm can be found in the user guide [9].

The comfort of the human is evaluated using Berkeley comfort model based on Zhang [10] and Zhang et. all. [11] [12] [13]. In the Berkeley model the body is divided into segments. Each segment local sensation is calculated based on the temperature of the core and skin. The sensation is quantified in a scale from -4 to +4, where -4 corresponds to a very cold sensation, 0 is neutral sensation and +4 is very hot sensation. The local sensation values are used to calculate overall sensation. Next local comfort is calculated for each segment based on the local and overall sensation. The comfort is quantified in a scale from -4 to +4, where the negative values correspond to uncomfortable state and positive values to a comfortable state. Finally the overall comfort is calculated. It is the average of the two most uncomfortable body segments with some additional conditions. If the right and left foot or the right and left hand are the two most uncomfortable segments then they are counted as one and the third most uncomfortable segment is included in the average. If the person has control of their environment for example the control of HVAC settings in the car, then it can be set in the comfort evaluation and the most comfortable segment will be included in the average. However if the two worst segments have local comforts below -2.5 instead the 3 most uncomfortable segments are used to calculate the average. The formulas are given below. The skin temperature is the skin temperature of segment and the skin set temperature is the temperature at which the sensation would be equal to 0. It is defined in a separate file and it is dependant on the clothing. The core temperature is obtained from the Pelvis segment.

$$S_{local} = f(T_{skin,i}, \frac{dT_{skin,i}}{dt}, \overline{T}_{skin}, \frac{dT_{core}}{dt}, T_{skin,i,set}, \overline{T}_{skin,i,set}) \tag{2.6}$$

$$S_{overall} = f(S_{lcoal}) \tag{2.7}$$

$$C_{overall} = f(S_{lcoal}, S_{overall}) \tag{2.8}$$

$$C_{overall} = f(C_{lcoal}) \tag{2.9}$$

3

Methods

In this chapter the models used for simulation are presented. Section 3.1 describes the solid parts composed of surface elements. In section 3.2 detailed information on the human model are provided. Section 3.3 describes the fluid parts used for convection and advection calculations. Section 3.4 describes how the localized heating is implemented in the system. Lastly section 3.5 provides insight on how the simulations are evaluated.

3.1 Cabin model

This work uses a CAD model previously prepared by the team at Volvo Cars. The model is divided into surface elements and represents the cabin of an SUV car. The model does not include the elements of the drive-train and the battery.

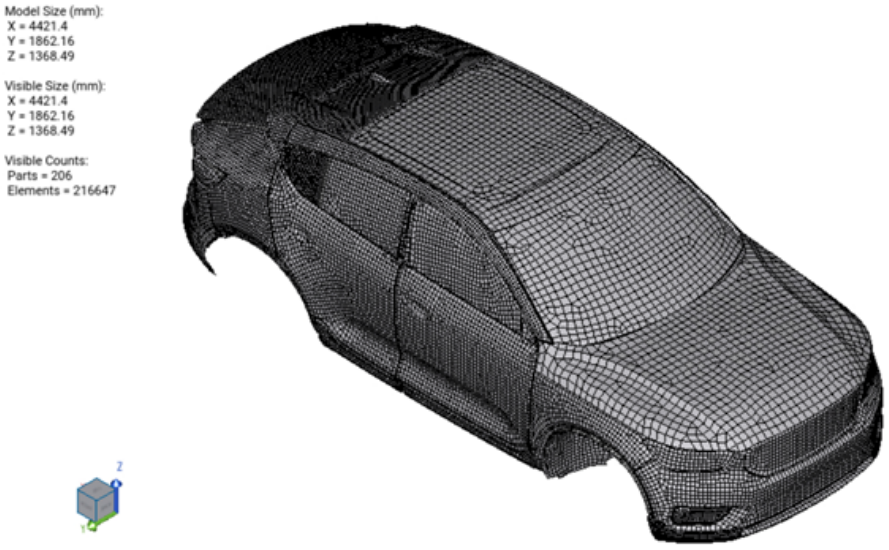

Figure 3.1: Car cabin model – Elements.

The car model is run in TAITherm software, made by ThermoAnalytics, Inc. This computer program specializes in thermal simulations. It calculates radiation, convection and conduction between the elements of the model.

The model consists of 216 647 shell elements. It is divided into parts and each part has a specified set of properties. These include: material, thickness, surface property and initial temperature. In case of multi-layer parts, the thickness and material are specified for each layer.

The surfaces elements are exchanging heat with other surface elements via radiation and conduction which is automatically calculated by TAITherm using the equations described in Section 2. The convection between the surface elements and the air nodes is described in section 3.3.

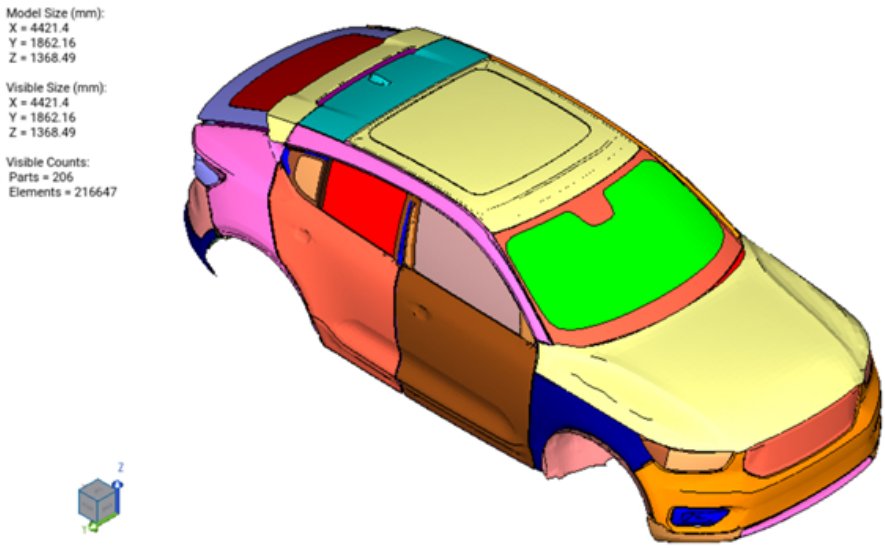

Figure 3.2: Car cabin model – Parts. Each part is marked by a distinctive color.

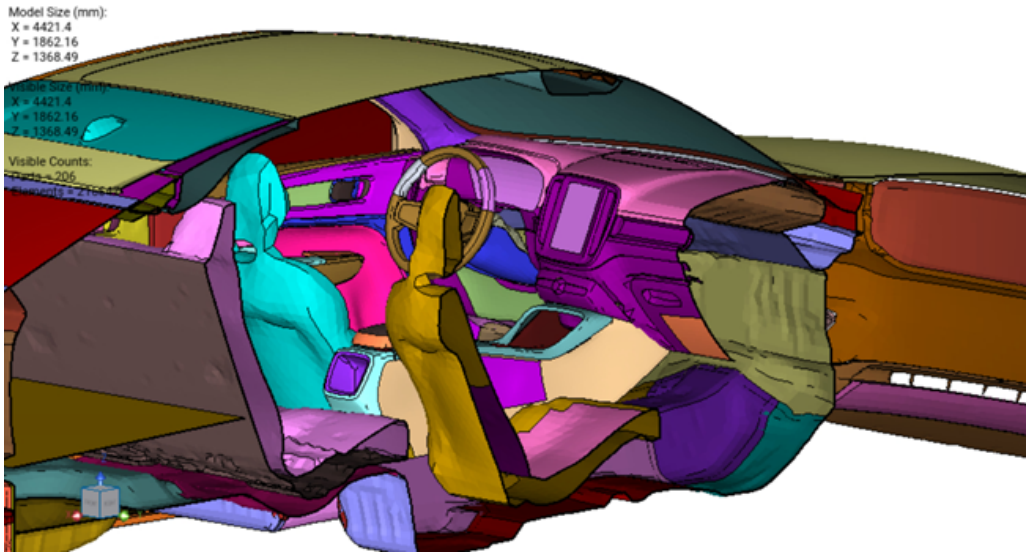

Figure 3.3: Car cabin model – A view inside the cabin. Section through the passenger's seat.

3.2 Human model

Beside the car itself a person (driver) is also a part of the simulation. In order to model the driver a manikin model is inserted. This manikin consists of multi-layer surface elements that model the ¨layers¨ in a human body such as skin, muscles, bones, internal organs etc.. The human model consists of 6609 surface elements grouped into 21 parts/segments, see figure 3.4. The manikin model represents a seated 50th percentile male based on Tiley [14]. During the simulation three versions of the human model are used. The first and second version are simulated in order to precondition the human model. Only the third version is simulated together with the car model in the actual cabin heat-up scenario. It is a procedure recommended by Thermo Analytics in order to obtain more realistic results from the comfort model. The skin temperatures and the comfort results are greatly affected by the state at which the human enters the cabin. First the human is assumed to be dressed lightly while seating in a comfortable environment for example at home or at the office. Second, the human is dressed in a warm winter jacket and walks outside to the car. Third still clothed warmly the human is sitting inside the car. Each version is simulated separately, and the subsequent version is initialized with the state of the human at the end of the previous simulation in order to start the simulation with realistic temperature distribution and initial comfort.

Figure 3.4: Human model – Elements (left), Parts (right)

Human body generates heat due to metabolic processes and work. For each version of the manikin an activity level is specified in Metabolic Equivalent of Task (MET) units. One MET is equal to 58.1 W/m^2. In all versions of the manikin the geometry represents a seated manikin. However, in the second version where the person is supposedly walking a parameter for the heat generation is set to ¨standing¨ which changes the heat distribution so that a higher percentage of heat is generated in the leg segments.

Figure 3.5: Person sitting in office. Left: outer layers. Right: number of layers.

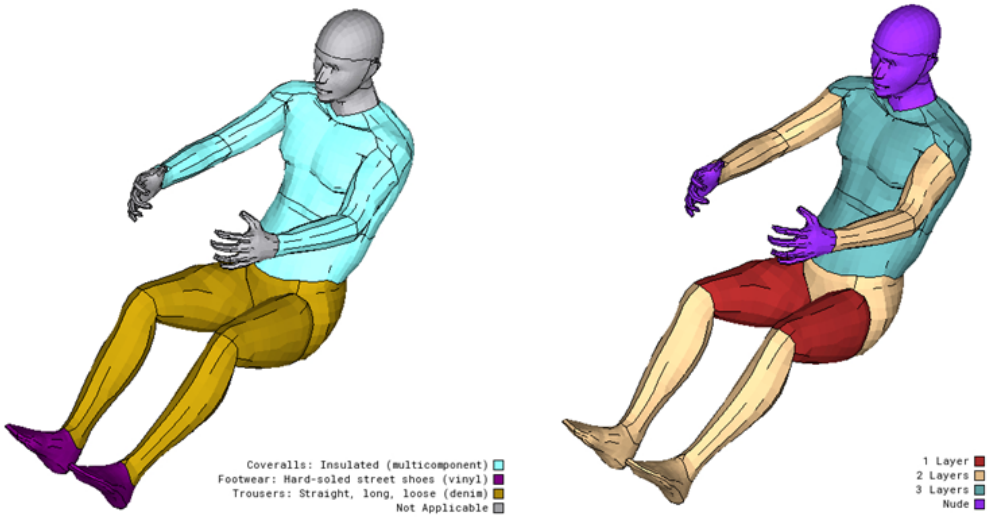

Figure 3.6: Fully dressed person. Left: outer layers. Right: number of layers.

The manikin layers are modified to cover the appropriate parts with clothing. In the first version the manikin is dressed in all clothes from the table 3.2 excluding nr 3 Coveralls, which corresponds to a winter jacket. This configuration is presented in figure 3.5. The second and third versions use the same clothing ensemble presented in figure 3.6. The clothing materials and their corresponding parameters are taken from the TAITherm database, the parameters influence the rate of heat transfer through the clothing layer. The materials are defined in a way that the thermal and evaporative resistance is based on the area of the surface irrespective of the thickness of the clothing layer. In calculation of the resistances the actual element surface area is multiplied by the local surface area factor.

In table 3.1 the conditions for each version are summarized.

Nr	Activity equivalent	Activity level (MET)	Activity type	Clothing insulation (CLO)
1	Sitting quietly	1.0	Sedentary	1.03
2	Walking	1.2	Standing	1.23
3	Driving	1.2	Sedentary	1.23

Table 3.1: Manikin summary

Nr	Clothing	Local surface area factor	Vertical Evaporative Resistance $[m^2 * kPa/W]$	Vertical Thermal Resistance $[m^2 * K/W]$
1	Underwear: T-shirt (knit)	1.094	0.0053	0.057
2	Sweater: Long-sleeve, round neck (thick knit)	1.133	0.0394	0284
3	Coveralls: Insulated (multicomponent)*	1.284	0.0239	0.253
4	Underwear: Briefs (knit)	1.083	0.0079	0.089
5	Trousers: straight, long, loose (denim)	1.444	0.0151	0.129
6	Footwear: Calf length dress socks (knit)	1.077	0.0417	0.075
7	Footwear: Hard-soled street shoes (vinyl)	1.429	0.079	0.222

Table 3.2: Clothing ensemble. *Represents the winter jacket, it is not included in the clothing ensemble for the first version of the manikin, when the manikin is preconditioned in the office environment.

3.3 Air node network

Additional to the surface elements, air nodes are inserted into the model in order to facilitate convection calculations. Air nodes are 1D elements representing a given volume of fluid. It is possible to simulate the cabin with just one air node representing the full volume of air inside it. However, this creates a spatially homogeneous distribution of fluid parameters. Advection connections between multiple air nodes can be used in order to create a network of air nodes which will model the distribution of the fluid temperature and corresponding heat exchange via convection. The aim is to approximate the flow field without a need of a full 3D simulation of the flow. Alternatively, it is also possible to couple an external CFD program with TAITherm. [7]

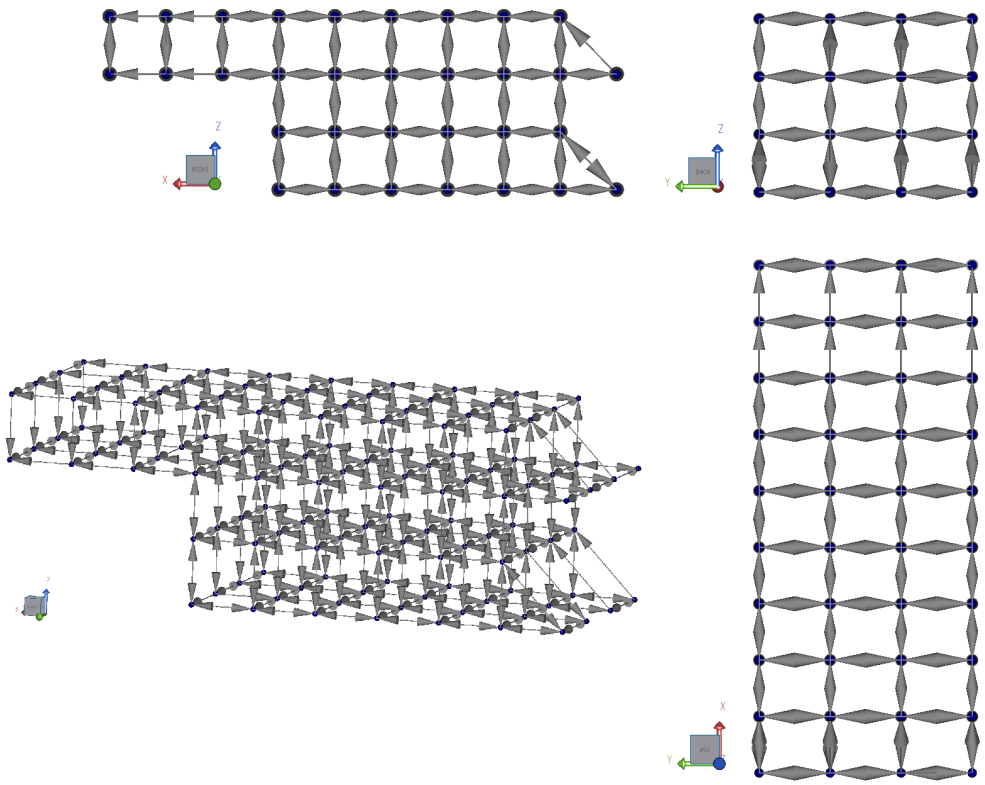

Figure 3.7: The air node network

In this thesis the network approach is used. The main goal of the thesis is to evaluate the effects and potential benefits of the localized heating components: radiant and conductive parts. This can be done In TAITherm without using the air node network. However, simulating the cabin without any ventilation at all would be unrealistic. In a real-life scenario most likely a combination of localized heating and classic HVAC will be used. Hence in order to provide an estimation on the effect of localized heating, multiple scenarios are simulated with varying boundary conditions. In order to quickly investigate a wide parameter range it is necessary to develop a model with short runtime. Thus running multiple 3D CFD simulations is not feasible. Therefore, a network of fluid air nodes and their advection links is made in order to approximate the flow field in the cabin and the heat input from the HVAC system. This approach is a compromise between the short runtime offered by a surface only simulation and the flow field accuracy provided by a 3D CFD simulation.

The network is generated using a sample CFD simulation provided by VCC, described by Anandh (Baseline configuration) [5], and a subvoluming macro courtesy of ThermoAnalytics. The macro divides the 3D flow field computed in STAR-CCM+ into subvolumes using an orthogonal grid. Each subvolume is represented by an air node. The steady-state advective fluxes between the nodes are determined from the CFD results, and are kept fixed throughout the simulation. The finished network consists of 128 air nodes, with each node having multiple advection connections to

the neighbouring nodes. Each nodes represents a volume of air of roughly 40 l. Some nodes are realistically less than 40 l since the volume overlaps with for example the seats, however, for simplicity it is assumed that all the nodes are equal in size.

While the network is a better approximation of the flow field than a single air node it is still far from the resolution provided by a full 3D CFD simulation. Additionally, the advection links are based on a single final timestep of a transient simulation, where it was run sufficiently long to reach conditions similar to a steady state. Moreover, the simulation did not include the manikin. However as mentioned before this is not a study of the flow field in the cabin and in order to reduce computation time these limitations are deemed acceptable.

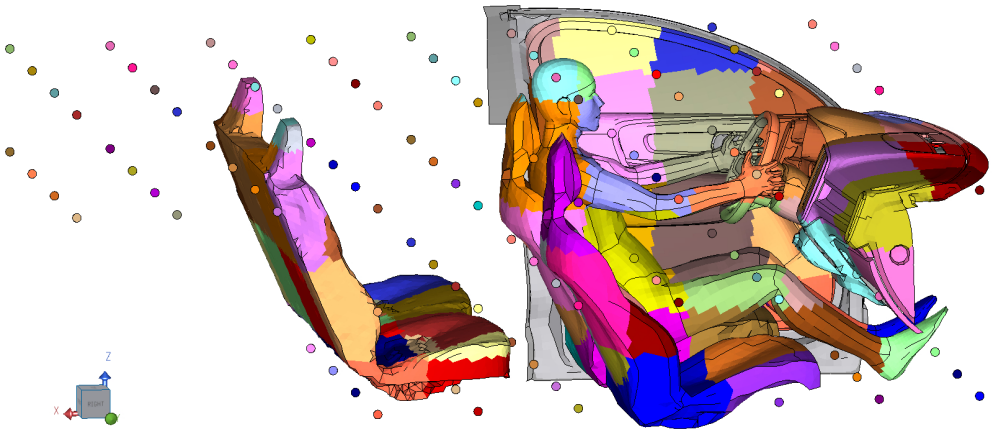

Figure 3.8: A view of the air nodes inside the cabin. Each fluid node has a different colour. The surface elements are coloured according to the node they are connected to. The advection connections between the nodes are hidden for a better visibility of the surfaces.

The surfaces in the cabin exchange the heat via convection with the nearest air nodes using the Newton's law of cooling. Each surface element has a specified convective heat transfer coefficient (h) and the fluid temperature is calculated at the fluid node that is closest geometrically. The manikin, some of the surrounding surfaces and their connections to the air nodes are shown in figure 3.8. Most of the surfaces inside the car have a convection coefficient h equal to 5, with exception of the floor, the interior side of the windshield, and the top side of the instrument panel, which have h = 3. The surfaces of the manikin have an automatic calculation of the h coefficient based on the TAITherm human convection library using the equation

$$h_{c,mix} = \sqrt{a_{nat}\sqrt{T_{sf} - T_{air}} + a_{frc}V_{air,eff} + a_{mix}}, \tag{3.1}$$

where $h_{c,mix}$ is the heat transfer coefficient, a_{nat} , a_{frc} , and a_{mix} are manikin coefficients for natural, forced, and mixed convection, they are included in the TAITherm library and are different for each body segment, $V_{air,eff}$ is the estimated velocity of

the freestream close to each body segment, see figure 3.9, T_{sf} and T_{air} are the surface and air node temperatures, respectively.

The free stream velocities close to each segment were estimated based on the mean velocities from the aforementioned CFD simulation (see figure 14 in Anandh [5]). Since the CFD simulation did not include the manikin the velocity values assumed for the manikin are subject to a considerable margin of error.

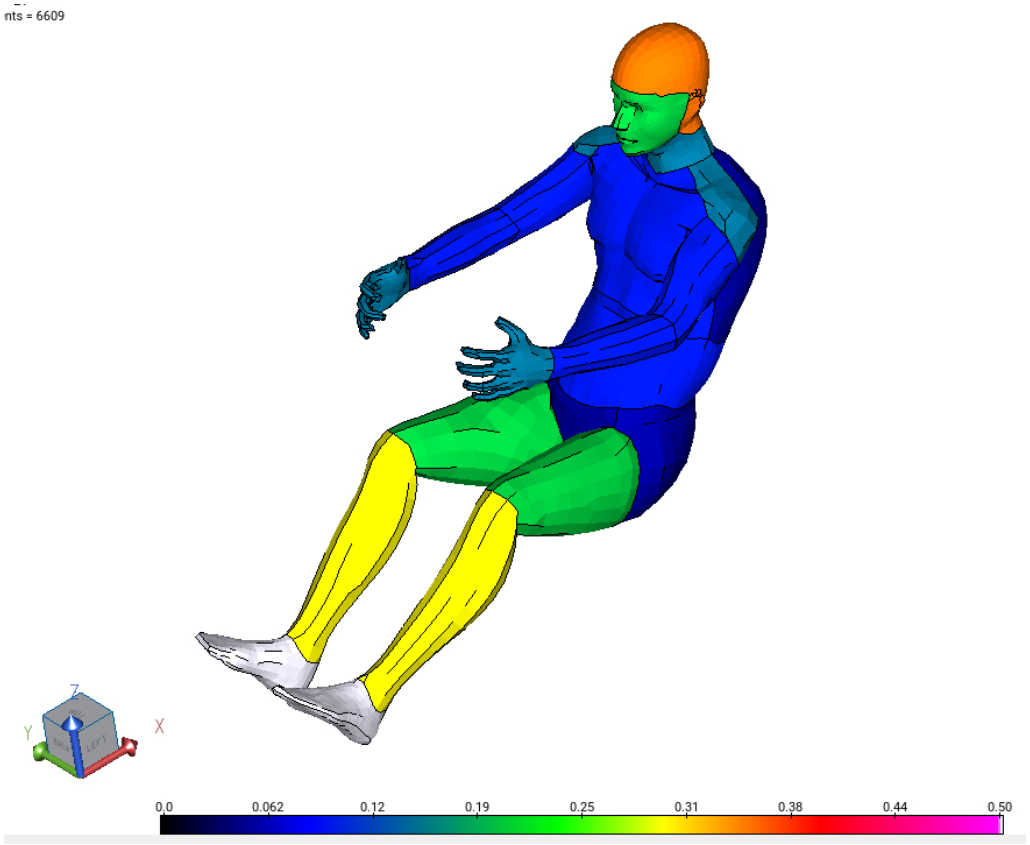

Figure 3.9: Air velocities on manikin front surfaces for convection calculations. Velocities in m/s.

3.4 Localized heating

In this thesis the localized heating is performed by two types of heated surfaces, radiant and conductive panels. The radiant panels are composed of resistive electrical wire enclosed in textile material and attached to the surfaces inside the cabin of the car. Under electrical load the wire heats-up and the heat from the hot panel is transfer to the human (mostly) via radiation. The conductive panels are constructed similarly but they are in direct contact with the human hence the heat is primarily exchanged via conduction. In order to model the heated surfaces some of the surface elements are modified. An additional layer is added to the surface elements and heat is imposed in between the new and the old layer modelling the

behavior of the heating component. A complete list of the panels is given in table 3.3 and in figure 3.10.

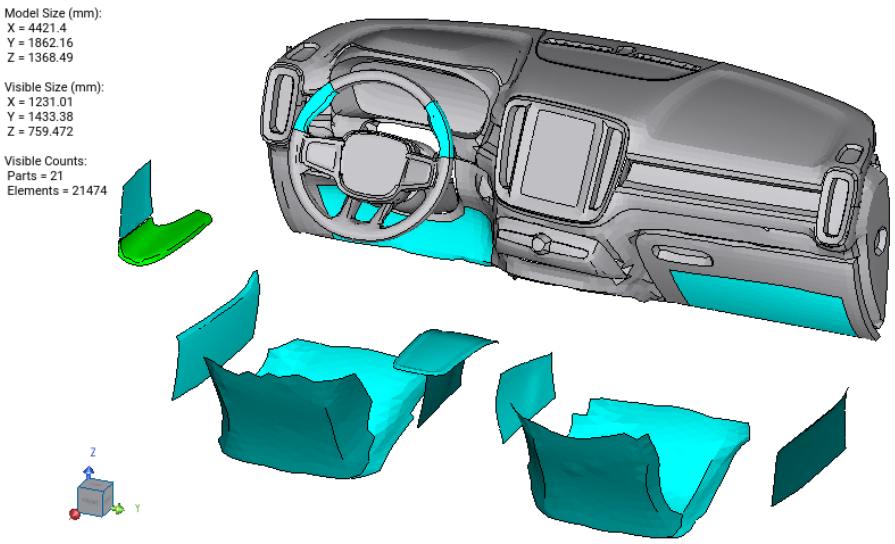

Figure 3.10: Inside of the cabin. Panels highlighted in color.

Nr	Part name
1	Panel under STW
2	STW C
3	Driver door panel bot
4	Driver door panel top
5	Driver armrest panel C
6	Driver seat cushion C
7	Driver seat back C
8	Driver tunnel panel
9	Tunnel panel C
10	Glovebox Panel
11	Front pax door panel bot
12	Front pax armrest panel C
13	Front pax tunnel panel
14	Front pax seat cushion C
15	Front pax seat back C

Table 3.3: List of panels. STW – steering wheel.

The surfaces marked with ¨C¨ in the list are meant to be in direct contact with the humans in the car. The temperature of these surfaces must be below a specified maximum in order to avoid burns. The mesh of the car and the mesh of the human model were created separately and thus the elements of the human model don't share edges with any other parts. Therefore the panels that are assumed to be in contact with the human model must be artificially connected with the human in

order to accurately capture conduction. This is done via thermal links feature of TAITherm as described in section 2.

A multitude of panels are created in order to facilitate future simulations, however for the purpose of the cases presented in this thesis, only the panels close to the driver are switched on. This includes panels 1, 2, 3, 4, 6, 7. Other panels are inactive. The rated power for panel under steering wheel (STW) is 110 W, for STW it's 10 W on each side. The driver bottom panel is 129 W and the top panel is 65 W. The seat cushion and back are both 114 W each.

When simulating the panels applying the constant power would result in very high temperatures of the heated surfaces. In reality some maximum temperature would be defined for each panel and it would be maintained with a controller by varying the amount of power supplied. In the program it is enforced using a simple java-script acting as a thermostat. While the temperature of the panel is below the parameter value, the script imposes the prescribed heat between the layers of the panel. The temperature is measured on a sensor which is the element that is geometrically in the center of each heated surface. At the end of each time step the thermostat checks the condition and sets the imposed heat for the next time step according to the formula

$$Imposed\ heat = \begin{cases} rated\ power, & T_{sensor} < (T_{param} - 0.5°C) \\ 0, & T_{sensor} > T_{param} \end{cases} \tag{3.2}$$

If the sensor element temperature is in between the two conditions then the thermostat state is conserved from the previous timestep. The code is presented in Appendix 1.

3.5 Design of study

The base cases were established by running a transient simulation without localized heating, using only HVAC to raise the temperature in the cabin and studying the comfort in each case. Those cases will serve as a baseline to compare against. Next the runs include localized heating in combination with HVAC with varying power levels. The comfort and energy usage is evaluated for each case.

The human comfort model returns an overall comfort value ranging from -4 to +4 with values above 0 corresponding to the person feeling comfortable. The time needed to reach and maintain overall comfort above 0 is denoted "time to comfort (TTC)". This together with power consumption is the main metric for success used in this project. A case is deemed successful if time to comfort is lower than 20 minutes. Out of the successful cases the ones with the lowest total power consumption are deemed the most optimal.

4

Results

In this section results from multiple simulation run will be presented. The simulations can be divided into three phases. In the next phase the end state of the simulation from the previous phase is taken as the initialization point. First phase is the simulation of only the human model sitting in the office in the comfortable environment. The manikin is stationary, relaxed, sitting. In the second phase it is also a manikin-only simulation. The person is walking from the office to the car. It is cold outside and before leaving the office the person puts on a winter jacket.

In the third phase there are many simulations but each is initialized with the state of the manikin from the end of the second phase. Additionally, in every simulation in the third phase the model consists of both the car cabin and the driver. In each simulation in this phase the car is moving at 50 km/h. The phases are summarized in the table 4.1. More details on the inputs are given in the section concerning the given case. At the end a comparison of the results is presented.

#	Simulation		Time [min]	Description
1	Office		30	Comfortable office environment, manikin only
2	Walking		2	Walking in -7 $°C$, manikin only
3	Cabin	Base cases	60	Only HVAC heating 3 cases
		Panel only	30	Only panel heating
		Batch 1	60	Combined heating 10 cases
		Batch 2	30	Combined heating 11 cases

Table 4.1: Overview of the simulation phases.

4.1 Manikin-only runs

Before the cabin simulation is run, the human model is preconditioned. The human model is put in an uniform environment at $22°C$ resembling an office or home. The model is run in transient mode for 30 minutes with a constant time step of 0.1 minutes. For the precondition cases the fluid velocities used for convection calculations are set to 0.05 m/s for every manikin surface. The resulting comfort

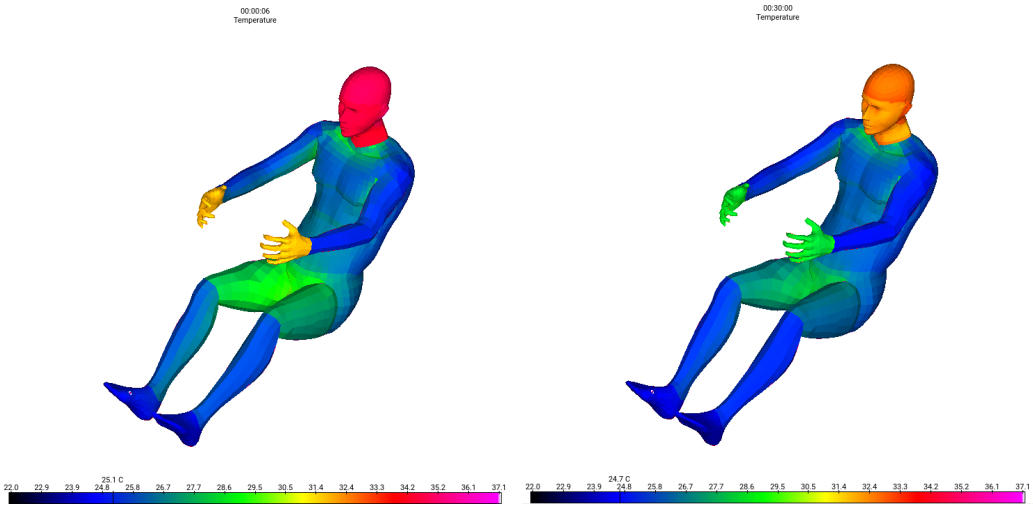

Figure 4.1: Surface temperature of the human in office. Left:At the first timestep of the simulation. Right: At the last timestep of the simulation.

is depicted in figure 4.2. The results are as expected for this run. The manikin is clothed warmly enough to be comfortable in the environment with prescribed temperature. Apart from the first few timesteps where numerical noise is present, the sensation in the first 5 minutes is around +1 indicating that the person feels slightly warm. Afterwards the sensation starts to drop to around 0 at 15 minutes mark. Since the temperature of the environment is constant, this reflects that the person is getting accustomed to the temperature. After 15 minutes the person is in a thermo-neutral state with the environment. At the same time the comfort is rising, from slightly above 0 in the beginning to +2 at around 17 minutes mark. The comfort then plateaus at +2 which is the maximum value that can be obtained for steady-state conditions in this comfort model. Additionally, the surface temperature of the model is illustrated in figure 4.1. Since this is only the surface temperature it doesn't give much insight into how the person is feeling. The only observation is that there is a slight but noticeable drop in skin temperature of the hands and head. A more insightful measure is the mean skin temperature and the hypothalamus temperature. They are plotted in figure 4.3. Here it can be noted that rate of change of mean skin temperature is high in the beginning but slows down later which roughly corresponds with the sensation results. The hypothalamus is a part of the brain which takes part in the human thermoregulation processes. It is roughly stable in this case at around $37°C$.

Since the comfort values are computed and available, the overall comfort will be used as the main metric in this thesis. This will facilitate comparison of different cases of the cabin simulations. Additionally, the overall comfort is a more complex and holistic measure than the aforementioned temperatures.

Next the conditions from the end of the previous simulation are used to initialize the second manikin simulation. This is done via a ¨Transient Restart¨ function in TAITherm. The manikin is now wearing a winter jacket and is put in the cold

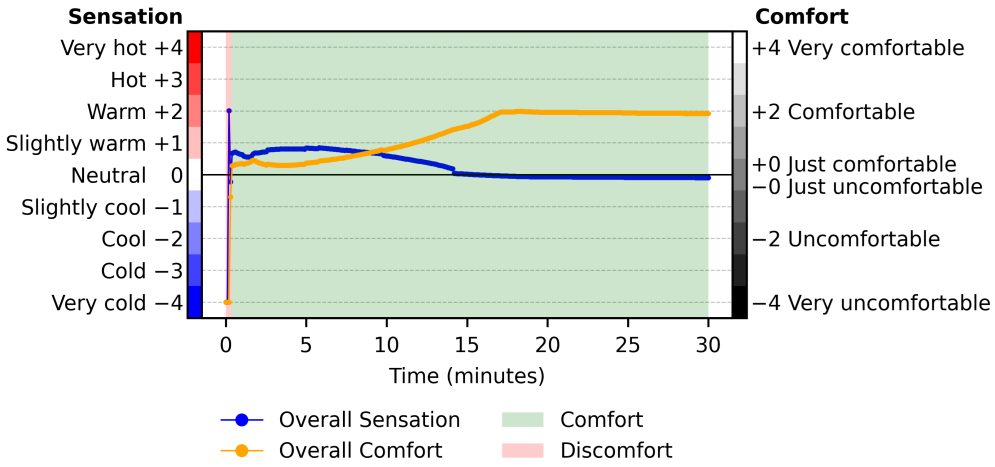

Figure 4.2: Man in office – comfort

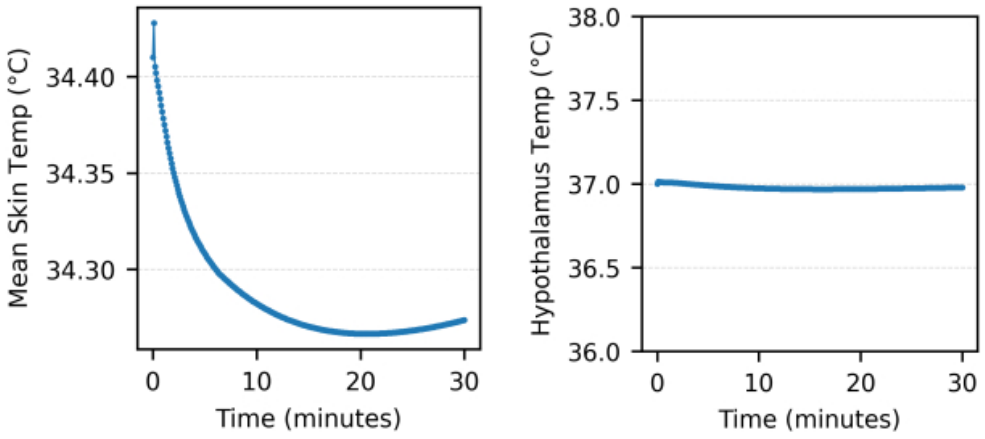

Figure 4.3: Man in office – important temperature measures

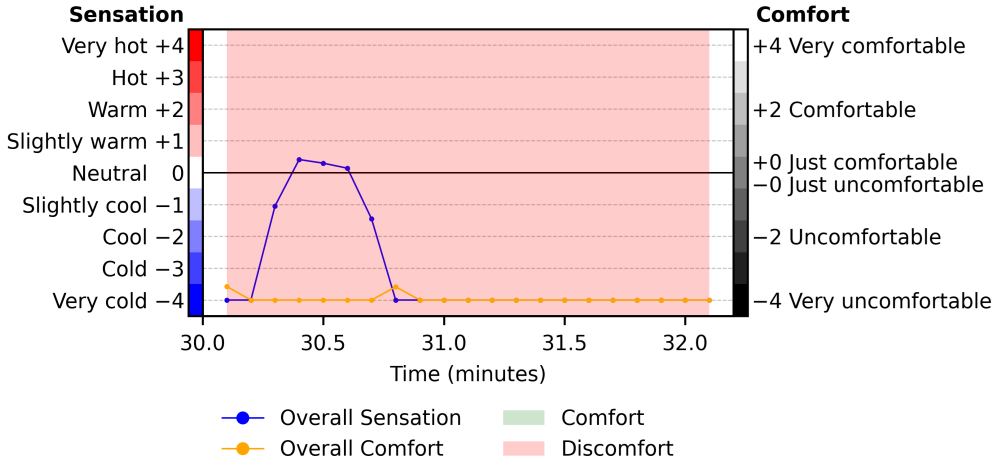

Figure 4.4: Man walking to the car – comfort

environment outside the office at -7°C. The model is run in transient mode for 2 minutes with a constant time step of 0.1 minutes. This aims to emulate the person walking from an office to the car that is parked outside. The resulting comfort is depicted in figure 4.4. Note that the time indicated in the graph includes the time that has passed in the previous model: human sitting in the office. This simulation starts at the end of the previous run +1 timestep.

As expected since the person moved from a comfortable warm environment to a very cold environment the comfort is very low for this simulation. An unexpected spike in sensation occurs at 30.2 minutes and lasts until 30.8 minutes. Upon checking the result files this corresponds to a sudden increase of local sensation (from -4 to +4) in some of the segments of the human, namely: Face, Chest, Back and Pelvis. it is not obvious why this occurs, however it may be due to instability of the human model arising from a sudden change of the environment's temperature. It is a known behaviour in the TAITherm software that when using a Transient Restart option, only one time step of data for some quantities is available to the next model. The equations used in the human comfort model rely on a time history of more than one time step, which can be the cause for the observed spike in sensation. However this is precisely why this preconditioning model is being run, so that similar behavior can be mitigated in the actual cabin simulation. After 31 minutes mark the sensation stabilizes, which is important as the end state will be used as an input for the next simulation.

4.2 Cabin simulation

After preconditioning the human model, the simulations are run with the car cabin model. It is assumed that before the driver enters the car, it has been soaked in the outside environment long enough that all of the parts have attained the same temperature. In the software it is done by setting the ¨initial temperature¨ of all of the car cabin part to ¨Bypass steady state¨ and -7°C. The human model is

initialized from the precondition model with the Transient Restart function. This means that the first timestep of the cabin simulation is at 32.2 minutes.

The interior convection is described in section 3. The exterior surfaces of the car are in convection with the outside air. The convection heat transfer coefficients are automatically calculated with an internal TAITherm library based on the model dimensions, outside air temperature set to -7°C, and flow velocity set to 13.88 m/s. This is equivalent to the car moving at 50 km/h. The library uses textbook flat plat formulas.

4.2.1 Base cases

In order to establish a reference point a few cases are run where only HVAC heating is provided and all the panels are in the off-state. These are called ¨base cases¨ and they are run in three power settings ranging from low to high heat scenarios. The exact power values are described in table 4.2.

The power is distributed to different air nodes in the cabin that are closest to the real location of the corresponding HVAC outlets. This is shown in table 4.3. Additionally, the power in the defroster is distributed 80% to the two central nodes and 10% to each side node. The power in the front vents is distributed 20% to the two central nodes and 40% to each side node. The four nodes corresponding to the front floor inlets get equal distribution, 25% each, the same is true for the rear floor inlets. The exact percentages in the distribution are chosen to match the values from the aforementioned CFD analysis [5]. The values are rounded to the nearest integer. Each of the base cases are run for 60 minutes. For the first 5 minutes of the simulation the time step is 6 seconds. Afterwards the time step is set to 15 seconds. The temperature of solids is shown in figures 4.5, 4.7, 4.9. The temperature of air nodes is shown in figures 4.6, 4.8, 4.10.

	Power	Unit
Base case 1	2500	W
Base case 2	3500	W
Base case 3	4500	W

Table 4.2: Base cases power

	Power	Unit
Defroster	22	%
Front floor inlets	36	%
Front vents	21	%
Rear floor inlets	21	%
Rear vents	0	%

Table 4.3: Base cases power distribution

4.2.1.1 Base case 1

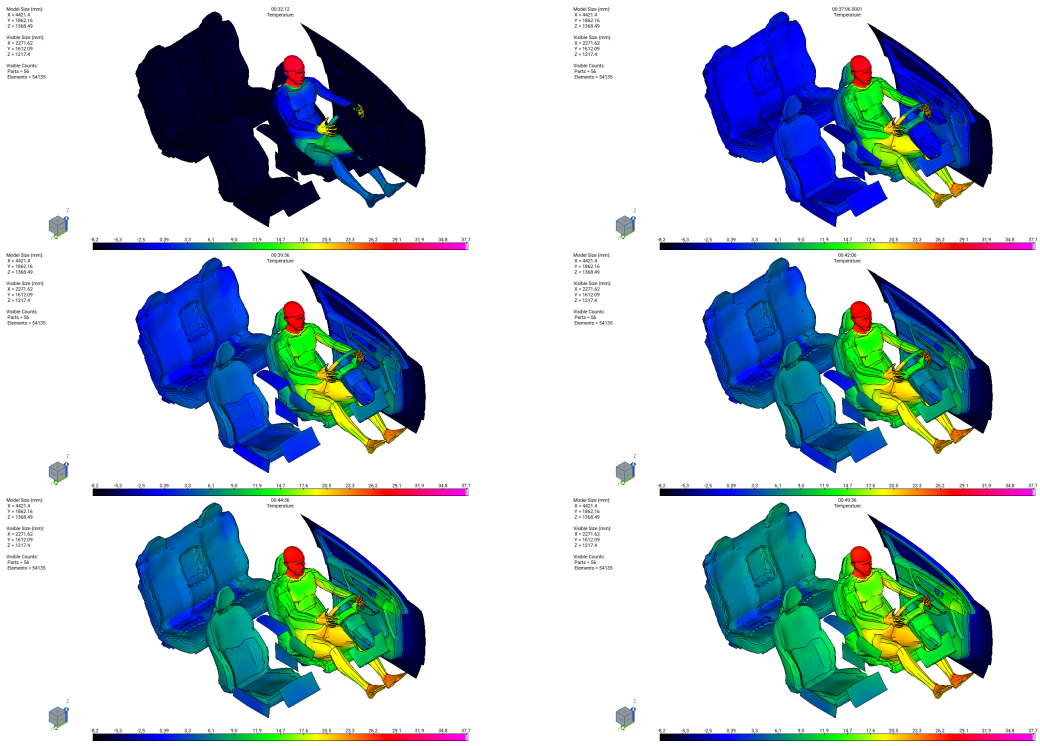

Figure 4.5: The temperature of selected surfaces in the cabin. From left to right and top to bottom: temperature after 0 min, 5 min, 10 min, 15 min, 20 min and 30 min.

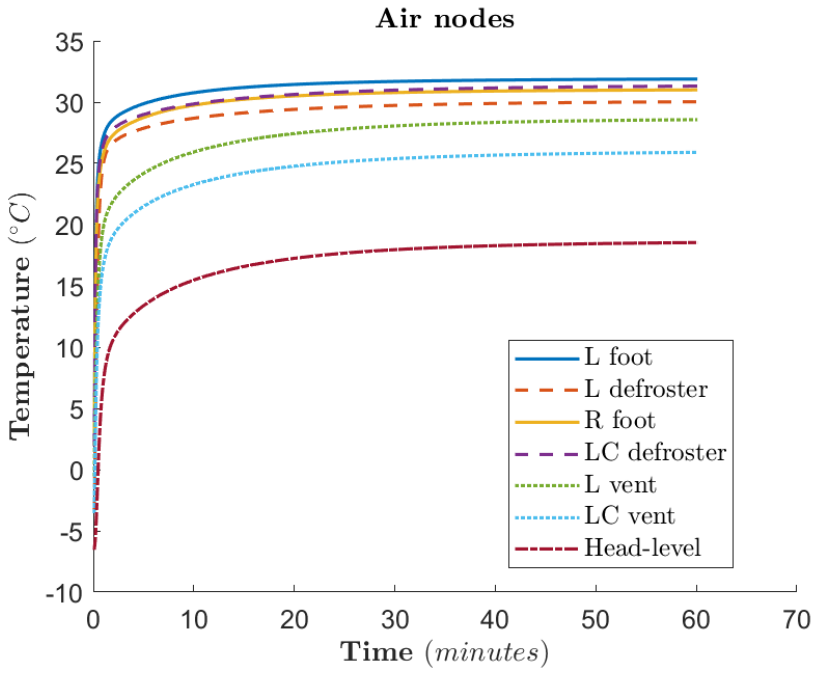

Figure 4.6: Base case 1 - temperature of interesting air nodes close to the driver.

4.2.1.2 Base case 2

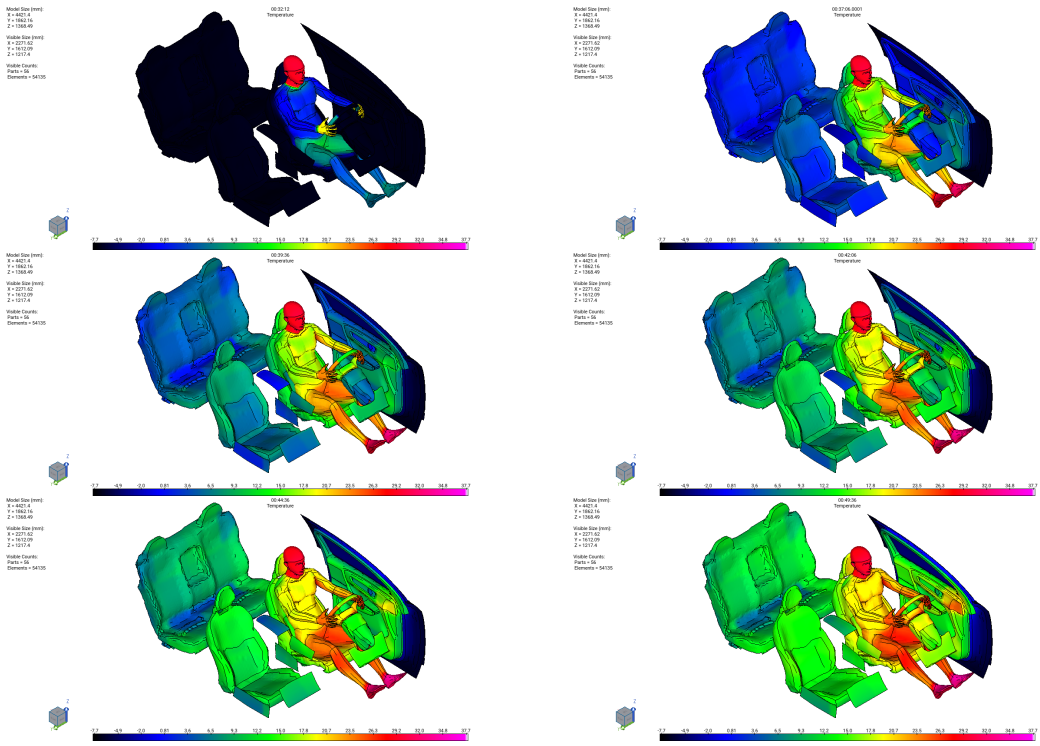

Figure 4.7: The temperature of selected surfaces in the cabin. From left to right and top to bottom: temperature after 0 min, 5 min, 10 min, 15 min, 20 min and 30 min.

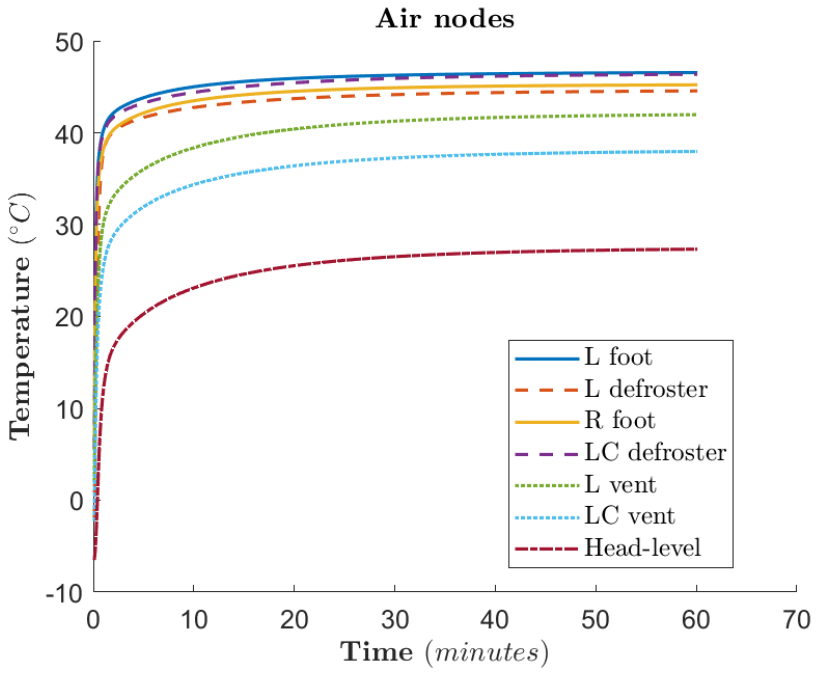

Figure 4.8: Base case 2 - temperature of interesting air nodes close to the driver.

4.2.1.3 Base case 3

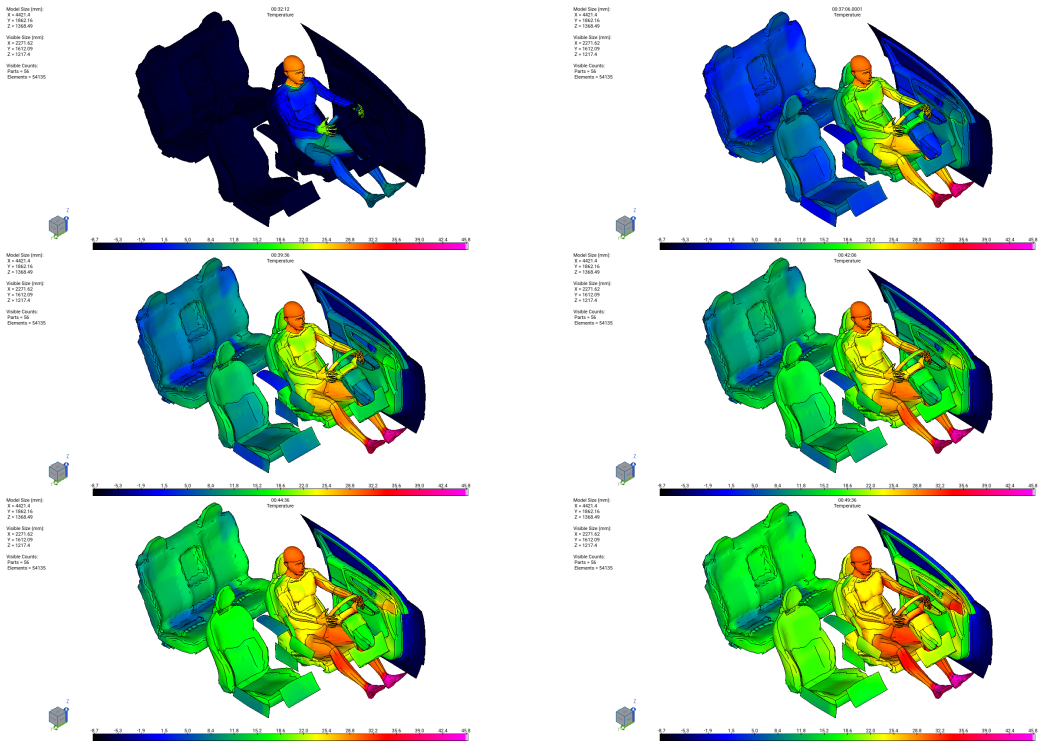

Figure 4.9: The temperature of selected surfaces in the cabin. From left to right and top to bottom: temperature after 0 min, 5 min, 10 min, 15 min, 20 min and 30 min.

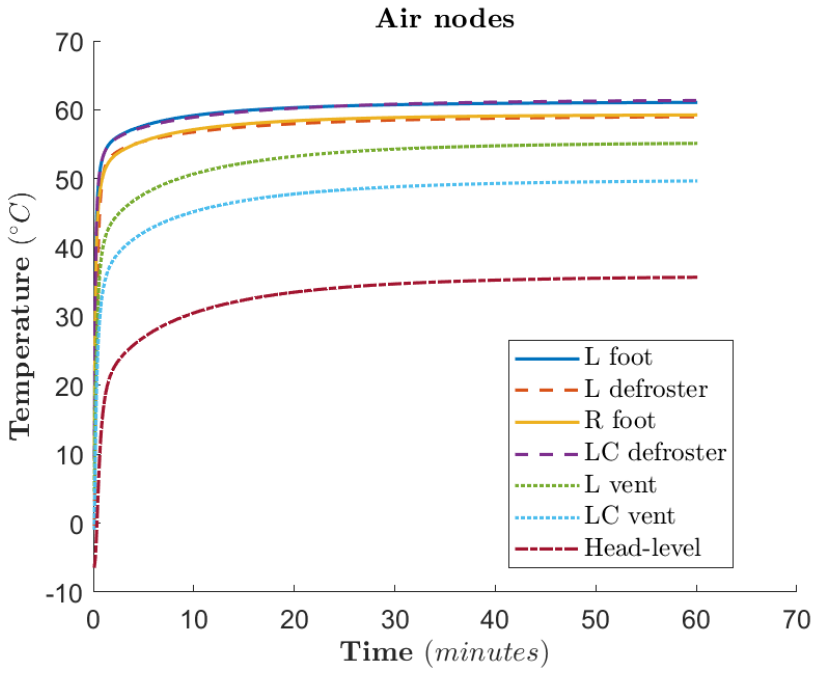

Figure 4.10: Base case 3 - temperature of interesting air nodes close to the driver.

4.2.1.4 Base cases comparison

In the three base cases different levels of comfort and sensation are reported. In cases with 2500 W and 3500 W a negative sensation level is maintained throughout the simulation, corresponding to cold sensation. In 4500 W case the sensation is initially cold but changes to hot after around 25 minutes. In the lowest power setting the comfort never reaches positive values. It is too cold for the driver to feel comfortable. For the case with the highest energy, initially a high level of comfort is exhibited until around 18 minutes mark. The temperature keeps rising over time and the driver starts to feel too hot, which also results in a feeling of discomfort. The case with 4500 W gives the best comfort in the first 20 minutes. The case with 3500 W gives better comfort after 20 minutes. The comparison between the cases is plotted in figure 4.11.

An interesting drop in comfort happens in base case 2 (3500 W) between 6.5 and 12.25 minutes. This corresponds to a slight drop in overall sensation. Upon closer inspection of the results this is mostly influenced by a drop in local sensation of the head and neck (the drop is more severe on the head segment). This is presented in figure 4.12. It is not trivial to discern whether this is an erroneous output or a proper calculation of the response from the physiological model. The sensation is compared to figure 4.13, the plot of temperature at an air node close to the head i.e. 'head-level temperature' of the air. The temperature of the air is rising quickly in the first few minutes, afterwards the rate of change diminishes in a logarithmic manner. The head and neck are one of the few segments that are not clothed, hence they are more susceptible to sudden changes in skin temperature and thus local sensation and comfort. Additionally, it is possible that the fact that the flow field is static in terms of velocity (advection links) might inaccurately result in a quicker initial rise in sensation than if the flow speed was starting from a stagnant condition and build up gradually. This may be influencing the observed behaviour of the sensation, however there is no conclusive evidence at the time of writing. In further analysis it is assumed that the comfort model results are accurate.

Each case has a time to comfort displayed in table 4.4. Here time to comfort is the time it takes to get to overall comfort above 0 and maintain it for a while. Therefore, even though the base case 2 reaches positive comfort after only 3.1 minutes, it is not counted since the comfort drops to negative values shortly after. Instead the time to the second instance of positive comfort is selected as then it is maintained. The base case 1 never reaches positive comfort hence it doesn't have a valid time to comfort.

	Time to comfort	Unit
Base case 1	N/A	min
Base case 2	12.5	min
Base case 3	2.0	min

Table 4.4: Base cases time to comfort

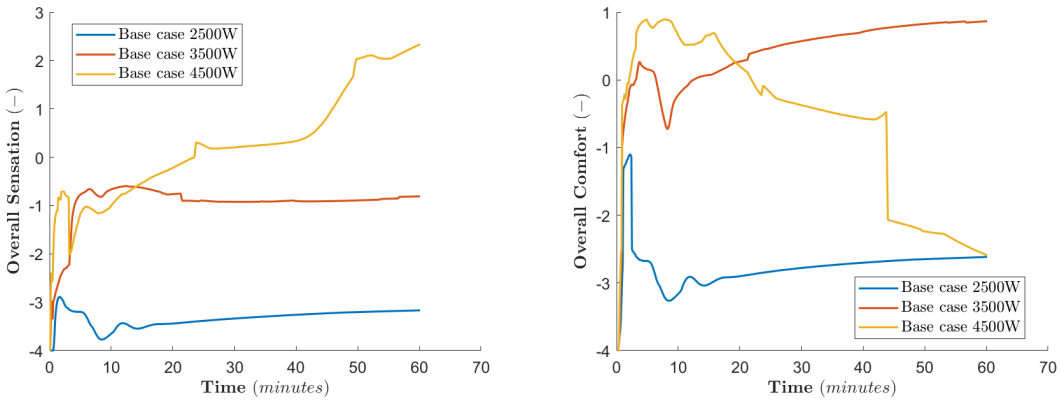

Figure 4.11: Sensation (left) and comfort (right) levels in the base cases

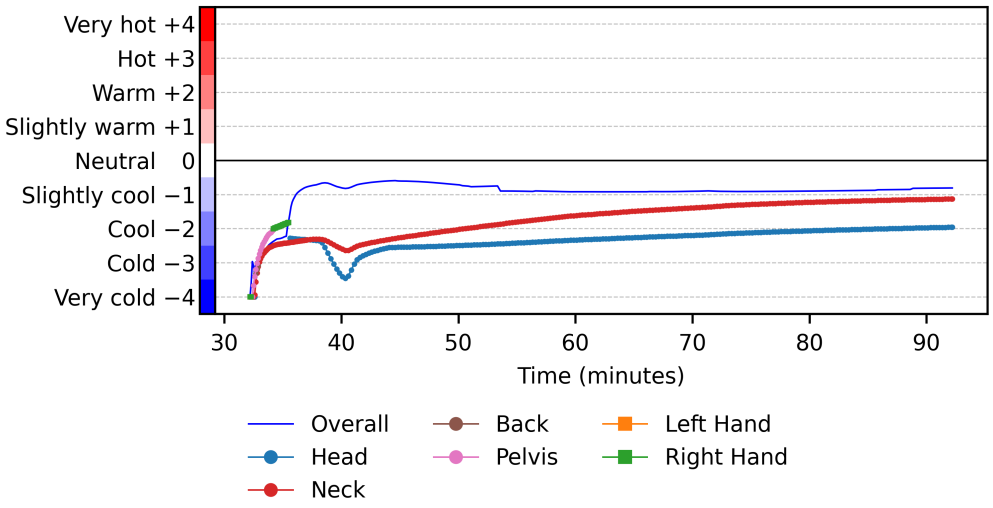

Figure 4.12: Base case 2 - the overall sensation and local sensation of the most uncomfortable segments of the body. Notice that in this graph the start of simulation is at 32.2 minutes.

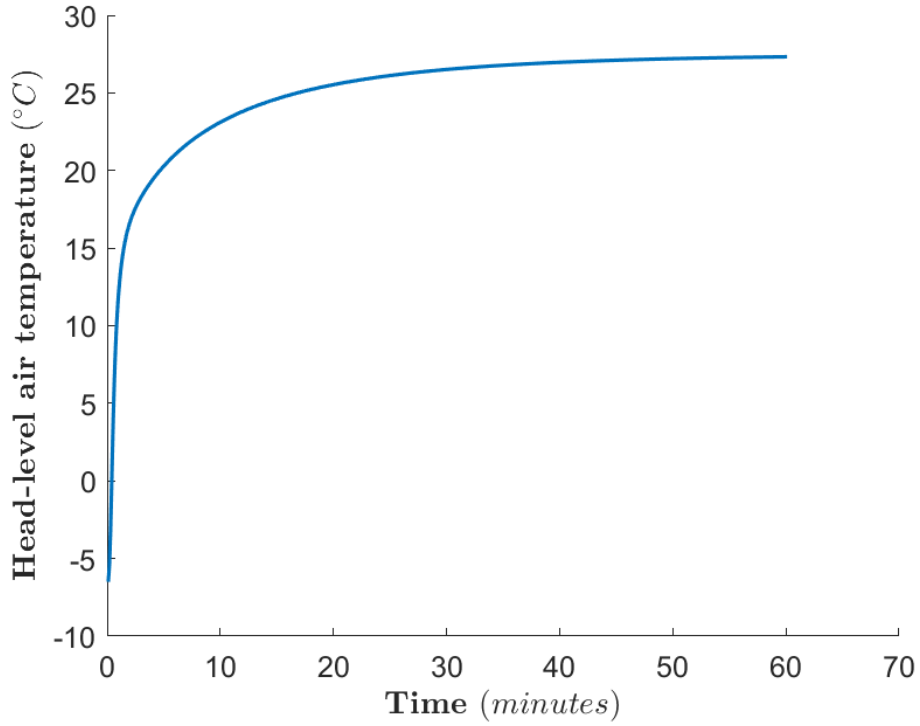

Figure 4.13: Base case 2 - The temperature of an air node that is close to the head of the manikin.

4.2.2 Only panels run

In this simulation run all of the HVAC air heating is set to 0 and the panels are set to the maximum safe values of temperature. The power supplied to the panels is described in the methods chapter and the maximum temperature is enforced using a thermostat script. The script is described in more detail in the next section and the code itself is attached in appendix A. In this run thermostat is set to switch the power in the panels to 0 when it reaches $50°C$ on the surface of conduction panels (seat and STW) and $80°C$ on the radiant panels. The simulation is run for 30 minutes. Other settings are the same as for the base cases. The results are as follows. The overall comfort and sensation of the manikin is presented in fig. 4.14

It is immediately clear that with the current setup of the panels even at the highest safe max temperature values it is impossible to achieve comfort in the given conditions without any air heating. The overall sensation of the manikin is -4 (very cold) throughout the simulation and the comfort initially rises from -4 to around -3.3 (very uncomfortable) for the first 8 minutes, after which it drops slowly to around -3.8 at the end. In figure 4.15 the energy usage of the radiation panels, conduction panels and total energy are plotted over time. Although the panels have constant power when switched on, since they cycle on and off after reaching the prescribed temperature the energy used is less than just power x time. Additionally it should be noted that the total energy used by the panels is just below 200 Wh after a

30 minutes cycle. so even at a high temp setting the panels use very little energy. The temperature of the panels is presented in figure 4.18 for easier visualisation of which panels are being heated up. It is observed that after 5 minutes the panels are already at the desired temperature and it is maintained afterwards indicating that the thermostat for the panels is working correctly.

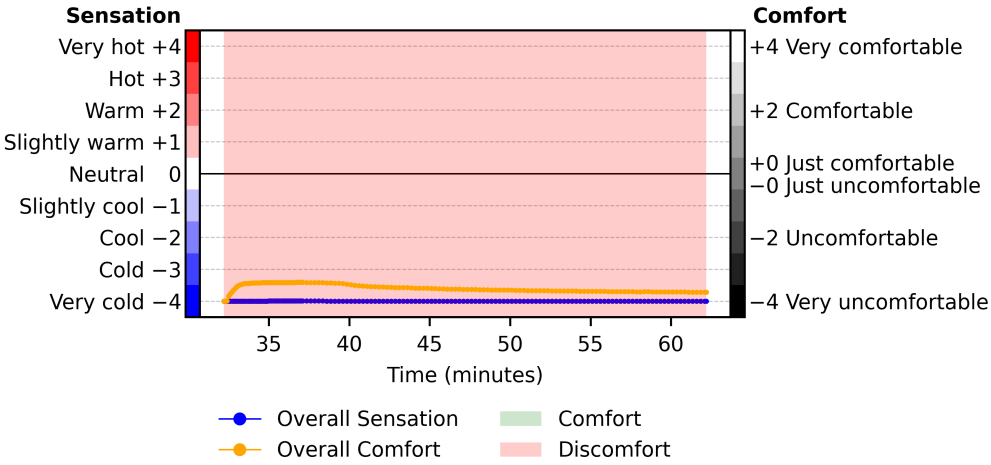

Figure 4.14: Comfort of the manikin with only panel heating. Notice that in this graph the start of simulation is at 32.2 minutes.

In figures 4.16 and 4.17 the temperatures of the selected surfaces in the cabin and the airnodes respectively are shown in the same manner that was presented in the base cases for ease of comparison. The heated surfaces are clearly hotter than in the base case, however the other surfaces remain at a low temperature throughout the simulation time. The surface temperature of the manikin is also low, much lower than in base case 1. As expected, since there is no hot air coming from the HVAC system the temperature of the air nodes remains low. The temperature of the air nodes rises slightly due to the convection with the hot surfaces and the manikin itself.

Taking into account the results of this run, in the next section the focus will be on achieving comfort with a combination of HVAC and panel heating.

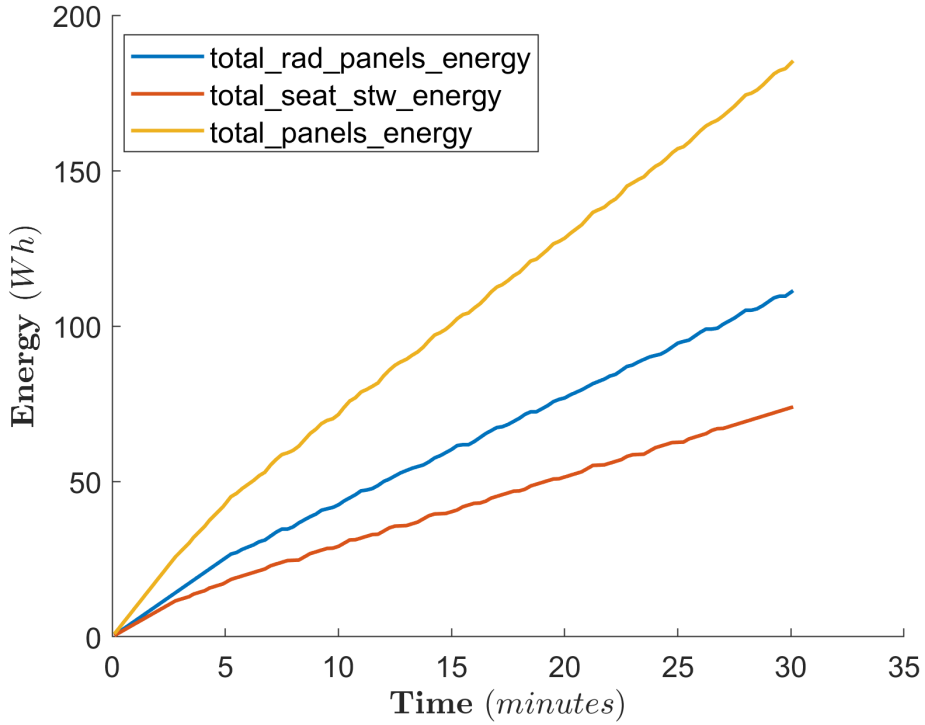

Figure 4.15: Cumulative energy usage of the panels over time.

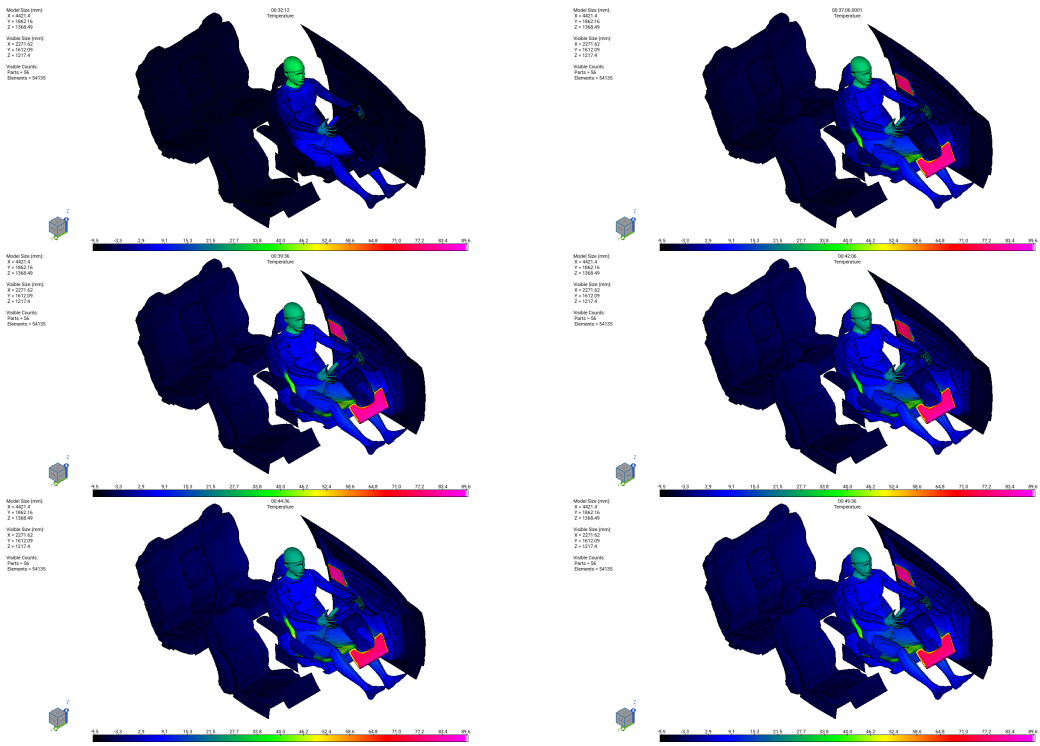

Figure 4.16: The temperature of selected surfaces in the cabin. From left to right and top to bottom: temperature after 0 min, 5 min, 10 min, 15 min, 20 min and 30 min.

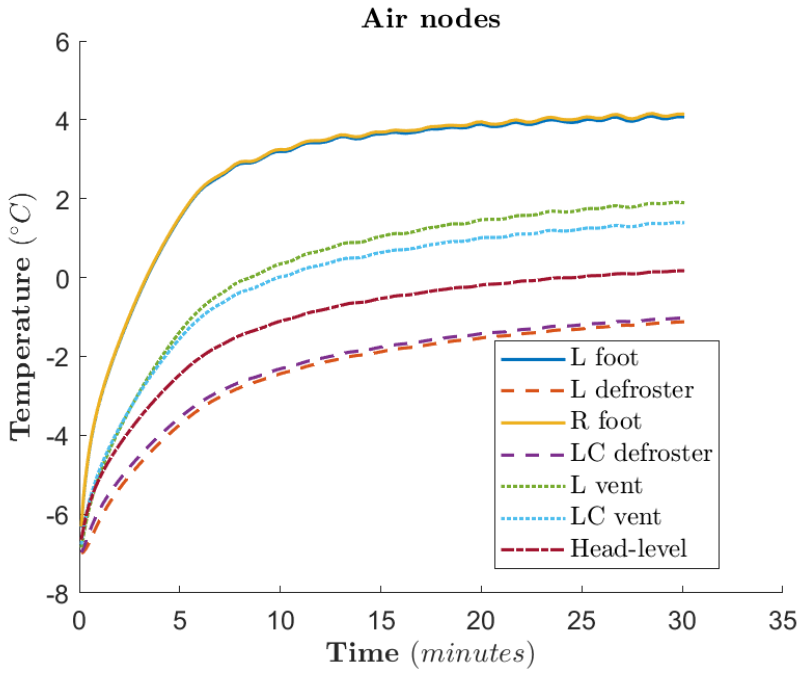

Figure 4.17: Panels only case - temperature of interesting air nodes close to the driver.

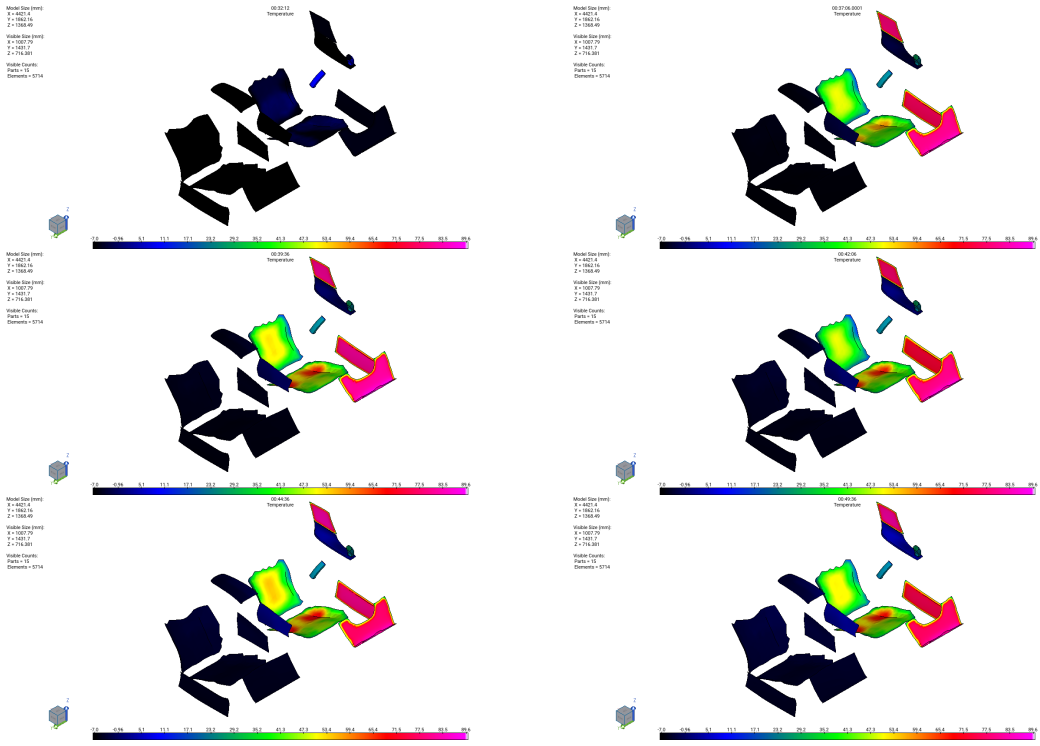

Figure 4.18: The temperature of the heated panels in the cabin. From left to right and top to bottom: temperature after 0 min, 5 min, 10 min, 15 min, 20 min and 30 min.

4.2.3 Parameter space - First batch

In order to test a wide range of boundary conditions in the cabin simulation a parameter space is defined. The parameters to be used are defined in the table 4.5. It includes a varied power level for the heated air in the HVAC system. Each heated surface has a defined power level, hence for the conductive surfaces i.e. the seat and the steering wheel and the radiative surfaces the parameter is the maximum temperature.

Parameter	Min value	Max value	Unit
HVAC heat	1000	5000	W
Seat + STW temperature	25	50	$°C$
Radiant panel temperature	40	80	$°C$

Table 4.5: Parameter space

In order to study the parameter space 10 cases are run. The parameters for each case are chosen using a ¨Latin hypercube¨ design of experiment method. This is done with a simple Python script. The cases generated are as follows:

1. Case 1 - HVAC = 1300 W, C = 20$°C$, R = 65$°C$
2. Case 2 - HVAC = 1700 W, C = 25$°C$, R = 50$°C$
3. Case 3 - HVAC = 2200 W, C = 30$°C$, R = 45$°C$
4. Case 4 - HVAC = 2500 W, C = 35$°C$, R = 80$°C$
5. Case 5 - HVAC = 2600 W, C = 50$°C$, R = 75$°C$
6. Case 6 - HVAC = 3200 W, C = 40$°C$, R = 55$°C$
7. Case 7 - HVAC = 3800 W, C = 45$°C$, R = 65$°C$
8. Case 8 - HVAC = 4000 W, C = 45$°C$, R = 60$°C$
9. Case 9 - HVAC = 4300 W, C = 30$°C$, R = 70$°C$
10. Case 10 - HVAC = 4800 W, C = 35$°C$, R = 40$°C$

where, HVAC stands for power in the HVAC system, C stands for max temperature in conductive surfaces (seat and STW), and R stands for radiant panels max temperature.

The sensation and comfort values are presented in figures 4.19 and 4.20 respectively. In cases 1, 2 and 3 even though a combination of HVAC and localized heating is active, there is not enough heat supplied to the driver and both the sensation and comfort metrics are very low. All of these 3 cases never achieve positive comfort.

In both case 4 and 5 a higher level of sensation is achieved reaching a peak value of around -1 (slightly cold). Both cases dip in overall sensation between 5 and 10 minutes marks. This is caused by a dip in local sensation of the head segment, similarly to what was observed in base case 2. The head sensation is plotted in figure 4.24. This is reflected in a sudden drop in overall comfort for both cases. In case 4 the comfort is low at around -2.5 (cold) at 10 minutes and slowly rises to -2 (cool) at 20 minutes where a sudden jump occurs to around -0.5 (slightly cool). Afterwards it remains oscillating around that value for the rest of the simulation time. Another segment that is unclothed are the hands of the manikin. Additionally the hands are in direct contact with the heated surfaces of the steering wheel. Due to the simple nature of the thermostat code it can cause violent oscillation in the hand sensation when cycling on and off. The data for the hand is plotted in figure 4.23. Both hand and head sensation levels stabilize at around 20 minutes mark which is the reason for the sudden jump in overall comfort. For case nr 5 the rebound to higher comfort happens earlier at around 13 minutes. This is due to a high level of comfort on the hands which itself is a result of higher parameter for the max seat and STW temperature. At around 30 minutes the comfort reduces sharply. This can be attributed to a very high sensation level on the hands as the temperature of the steering wheel keeps rising. The significant discomfort of the hands lowers the overall comfort. Both cases never reach positive comfort.

Case 6 quickly rises up to around -1 (slightly cool) in overall sensation. This yields slightly positive comfort at 3.5 minutes but drops to negative values at 6 minutes, due to the drop in the head local comfort. Afterwards the comfort rises back to positive values. The time to comfort is then 11.4 minutes. This is approximately 1.1 minutes faster than base case 2. In a 30 minutes scenario case 6 has used 1701 Wh of energy (plot in figure 4.21) which is 49 Wh less than base case 2. The energy usage over time is plotted by the lines in figure 4.22

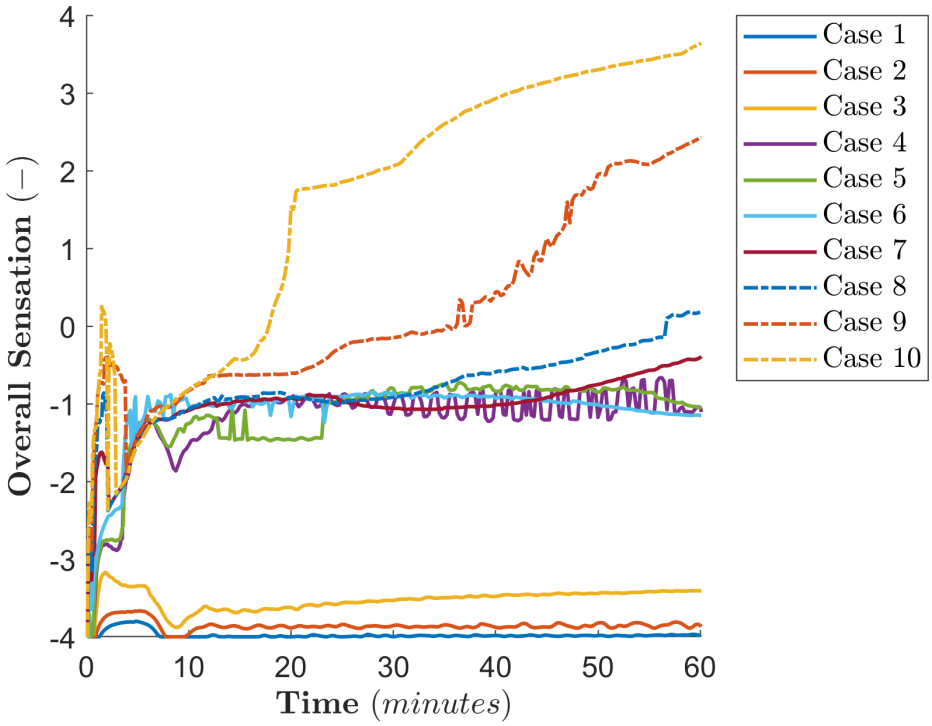

Figure 4.19: Comparison of overall sensation against time.

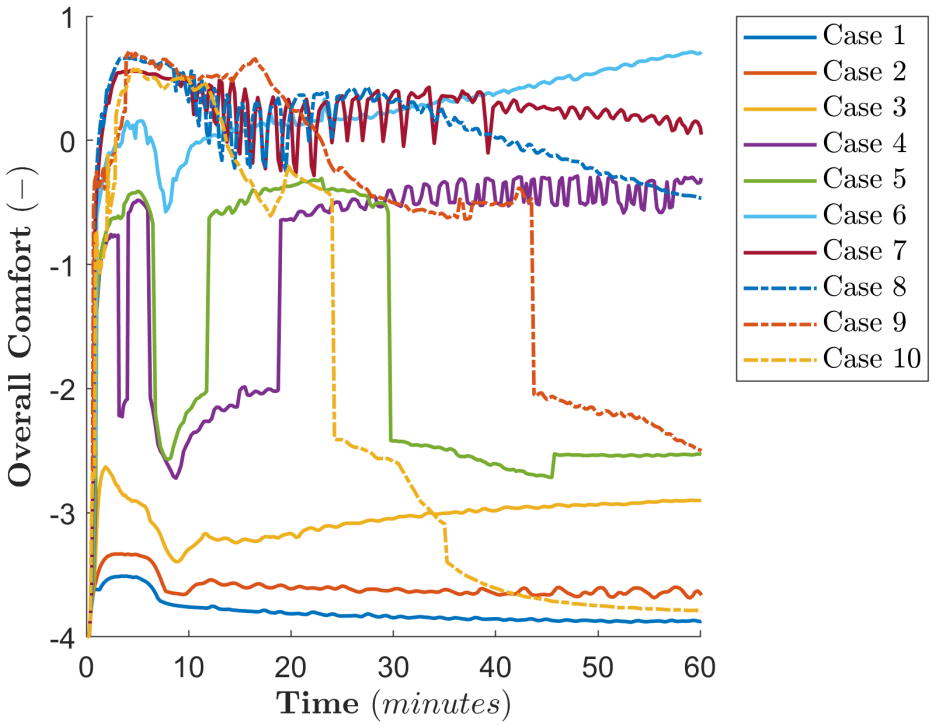

Figure 4.20: Comparison of overall comfort against time.

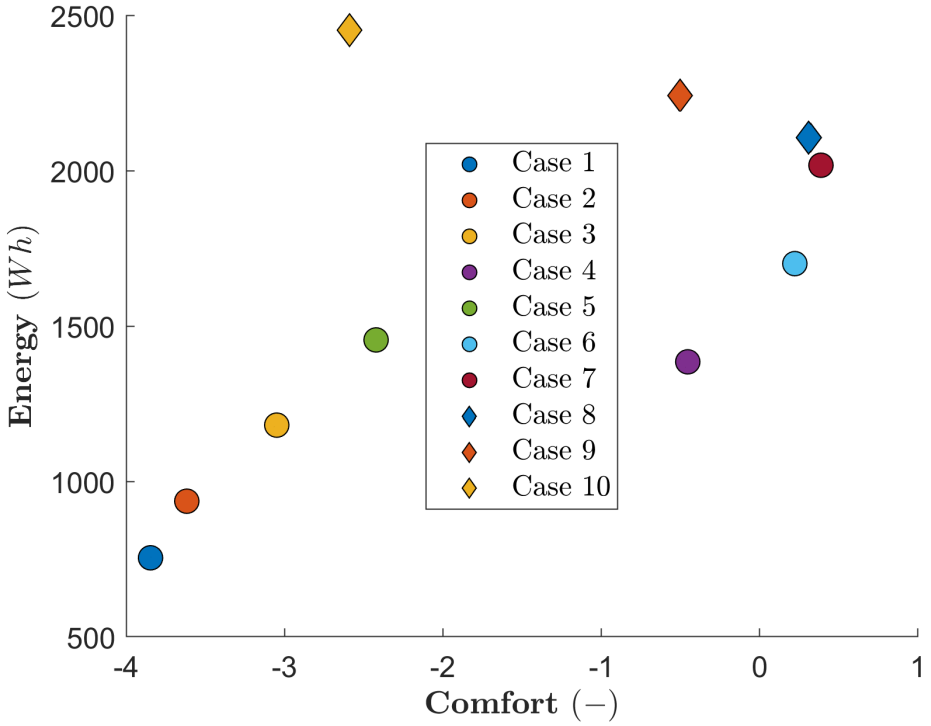

Figure 4.21: Comparison of total energy spent against comfort after 30 minutes of heat-up.

Case 7 and 8 both reach positive comfort very quickly. Case 7 has time to comfort equal to 1.4 minutes and in case 8 TTC is 1.2 minutes. Both cases exhibit violent oscillations in comfort due to the sudden switches of the thermostat action on the steering wheel influencing the hands local sensation and comfort. Due to the oscillation the overall comfort is reaching slightly negative values at some timesteps (-0.3 at the lowest point). However this can be considered as noise since the data follows a trend that remains positive throughout the oscillations. Using a smaller timestep and/or a more sensitive thermostat code would smooth out the oscillations. Considering that, the instantaneous negative values of comfort are not taken into account when establishing TTC for those cases. In a 30 minutes cycle case 7 uses 2017 Wh of energy and case 8 uses 2107 Wh. The closest reference is base case 3 which uses 2250 Wh and has TTC of 2.0 minutes.

Case 9 has TTC of 3 minutes and case 10 TTC is 2.8 minutes. However due to a high amount of energy entering the cabin in both cases the sensation keeps rising up to levels that are detrimental to comfort. In case nr 9 the overall comfort turns negative after 22.9 minutes and in case 10 after 13.65 minutes. Case 9 uses 2242 Wh of energy in a 30 minutes heat-up scenario and case 10 uses 2452 Wh. The closest reference case is base case 3.

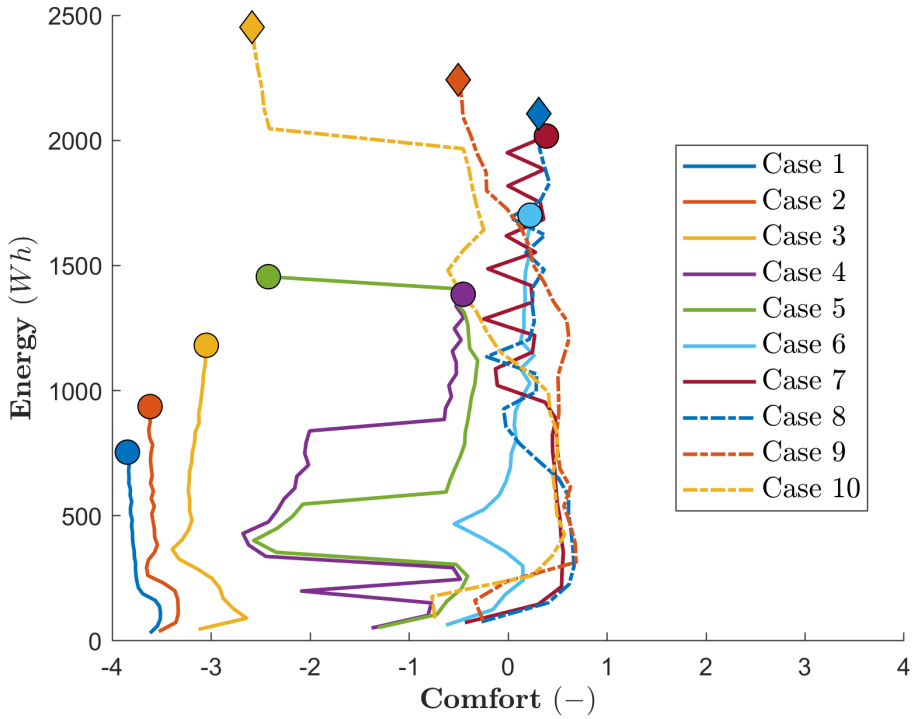

Figure 4.22: Comparison of total energy spent against comfort during the first 30 minutes of heat-up. The line plots the time history of each case.

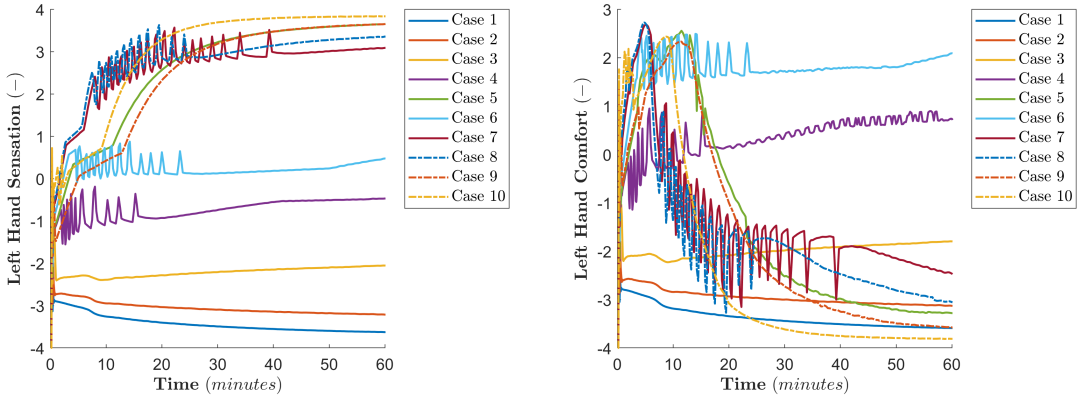

Figure 4.23: Comparison of hand sensation (left fig) and comfort (right fig) against time, using left hand data.

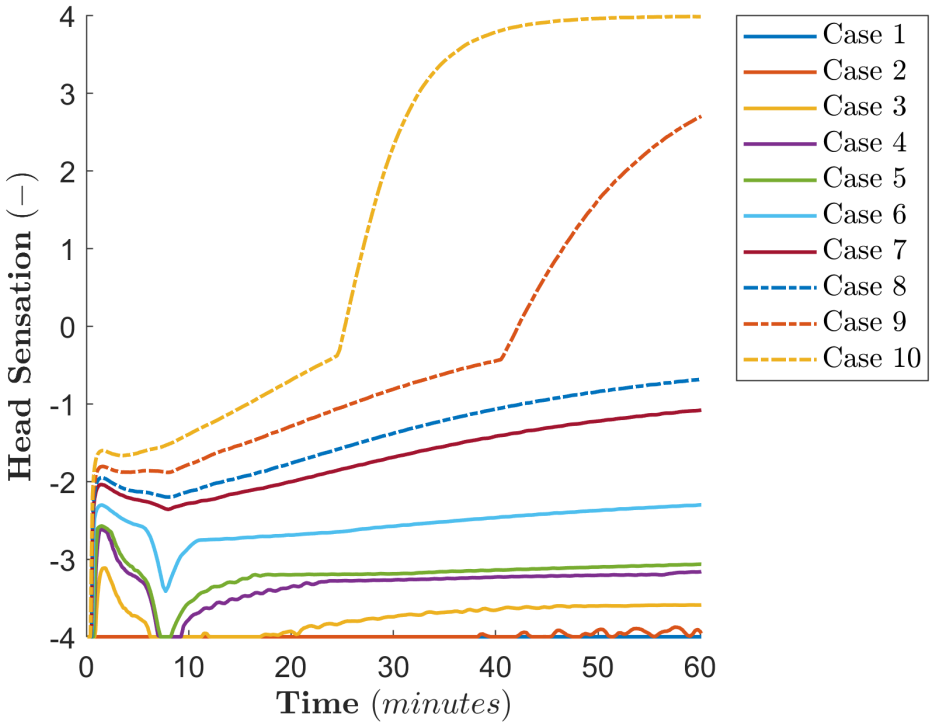

Figure 4.24: Comparison of head sensation against time.

4.2.4 Parameter space - Second batch

After reviewing the results from the first batch of simulations there were 2 clear conclusions. Firstly, cases 1-5 with the power settings for the HVAC closer to the lower bound all gave unsatisfactory results i.e. not reaching positive overall comfort. The cases with very high HVAC energy are achieving short TTC but afterwards rebound into negative comfort due to too much heat.

Secondly, the hand segments are sensitive to heat inputs and thus influence the overall comfort greatly. Since the hands are connected to the steering wheel with a conduction thermal link, the heat input on the STW should be tuned to be less invasive. This is done by reducing the maximum temperature on the steering wheel.

In order to further study the behaviour of the system and find a more optimal case the parameter range was narrowed down, the range for the second batch is shown in table 4.6. The HVAC range is reduced accordingly to previous observations. The parameter space for seat thermostat maximum temperatures is shifted to lower values and additionally the steering wheel thermostat max temperature is modified according to the formula

$$T_{max,STW} = 0.7 * T_{max,seat} \tag{4.1}$$

This aims to reduce the adverse impact of excessive steering wheel heating on the overall comfort. Finally the radiant panel parameter space remains the same as in previous batch, since the radiative panels are not effective in lower temperatures and higher temperatures are excluded due to health and safety concerns.

Parameter	Min value	Max value	Unit
HVAC heat	2600	3600	W
Seat temperature	10	40	$°C$
Radiant panel temperature	40	80	$°C$

Table 4.6: Parameter space

Eleven points for simulation are generated. Additionally, the simulation time is reduced from 60 minutes to 30 minutes. The points for the cases in the second batch are as follows:

1. Case 11 - HVAC = 2600 W, Seat = 35$°C$, STW = 24.5$°C$, R = 50$°C$
2. Case 12 - HVAC = 2700 W, Seat = 25$°C$, STW = 17.5$°C$, R = 65$°C$
3. Case 13 - HVAC = 2800 W, Seat = 15$°C$, STW = 10.5$°C$, R = 80$°C$
4. Case 14 - HVAC = 3000 W, Seat = 15$°C$, STW = 10.5$°C$, R = 75$°C$
5. Case 15 - HVAC = 3000 W, Seat = 25$°C$, STW = 17.5$°C$, R = 70$°C$
6. Case 16 - HVAC = 3100 W, Seat = 10$°C$, STW = 7$°C$, R = 40$°C$
7. Case 17 - HVAC = 3200 W, Seat = 30$°C$, STW = 21$°C$, R = 60$°C$
8. Case 18 - HVAC = 3300 W, Seat = 20$°C$, STW = 14$°C$, R = 70$°C$
9. Case 19 - HVAC = 3300 W, Seat = 30$°C$, STW = 21$°C$, R = 45$°C$
10. Case 20 - HVAC = 3400 W, Seat = 35$°C$, STW = 24.5$°C$, R = 60$°C$
11. Case 21 - HVAC = 3600 W, Seat = 40$°C$, STW = 28$°C$, R = 50$°C$

The results from these cases are summarized in the plots below.

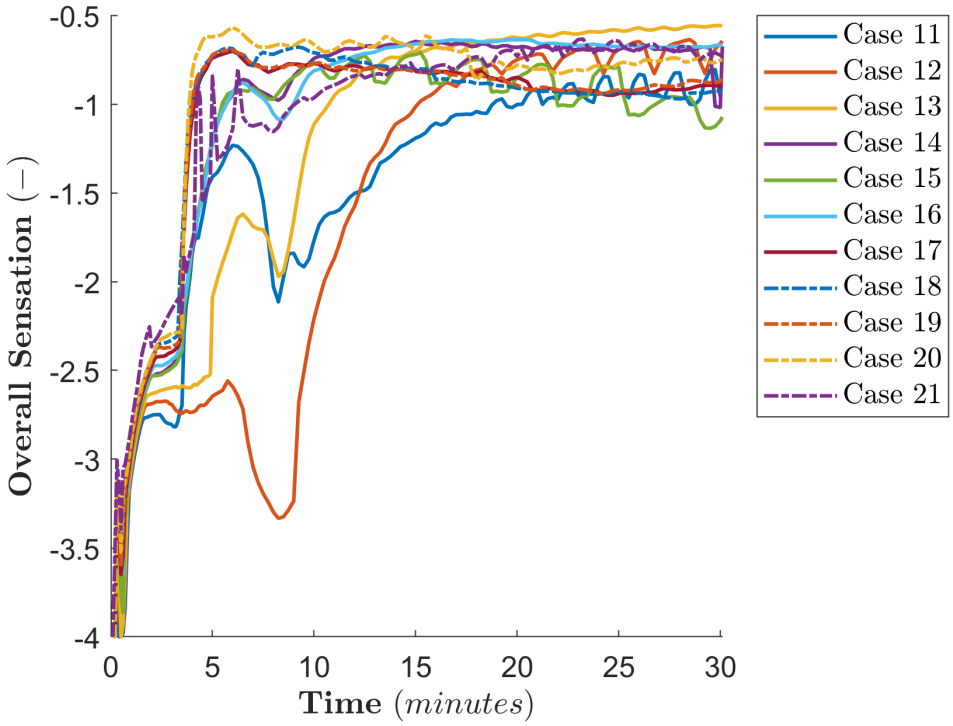

Figure 4.25: Comparison of overall sensation against time.

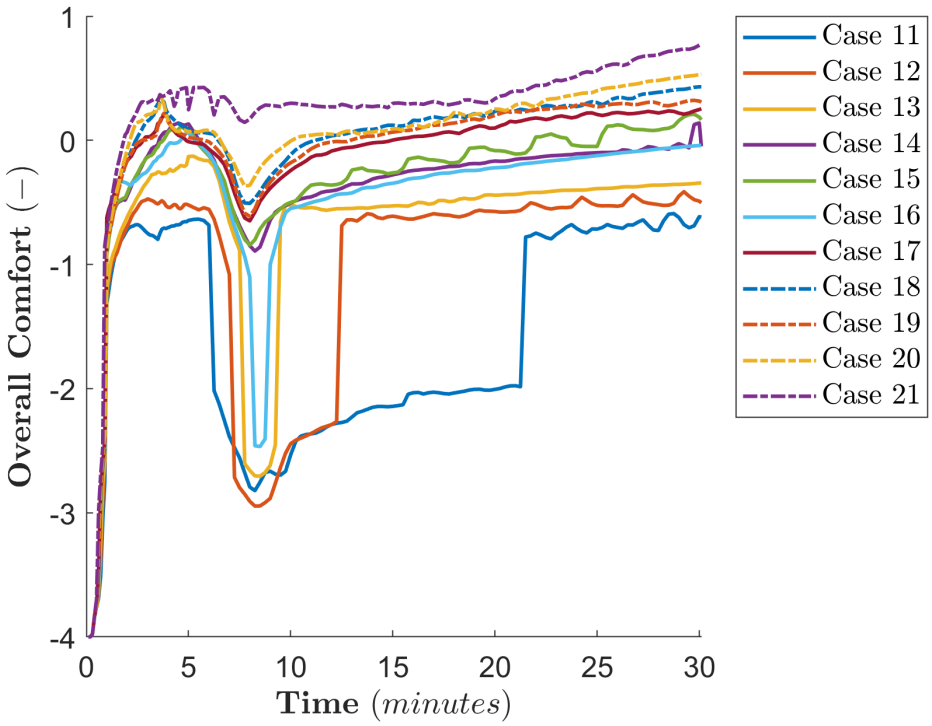

Figure 4.26: Comparison of overall comfort against time.

The rise of the overall sensation (fig. 4.25) in the beginning of the simulation is noticeably slower compared to batch 1. This is due to the slower rise in hand sensation (fig. 4.29), as expected from the introduced modification to the steering wheel temp. It is worth noting that in this batch all of the cases experience the severe drop in head sensation at around 8 minutes (see fig. 4.30), which has an extreme impact on overall comfort. It is the same behaviour as described in the base case 2.

Case 11, 12 and 13 never attain positive values for overall comfort (fig. 4.26). Case 14 is just comfortable (+0.1) between 3.4 and 5.4 minutes but the comfort is not maintained. Similar behavior is observed in cases 15 and 16. Case 17 similarly attains positive comfort between 2.7 minutes and 4.7 minutes, but after the drop it raises again to positive comfort and maintains it, giving it a TTC of 14.9 minutes, the energy usage in a 30 minutes cycle is 1690 Wh (fig. 4.27).

The same trends is observed in case 18 with TTC equal to 11.15 minutes. Case 18 uses 1719 Wh. Case 19 has TTC of 12.9 minutes and 1740 Wh, and for case 20 TTC is 10.15 minutes and energy is 1796 Wh. Case 21 is the only case which maintains positive comfort after reaching it for the first time. It has a TTC of 1.8 minutes and uses 1887 Wh of energy in 30 minutes. The energy usage over time is plotted by the lines in figure 4.28

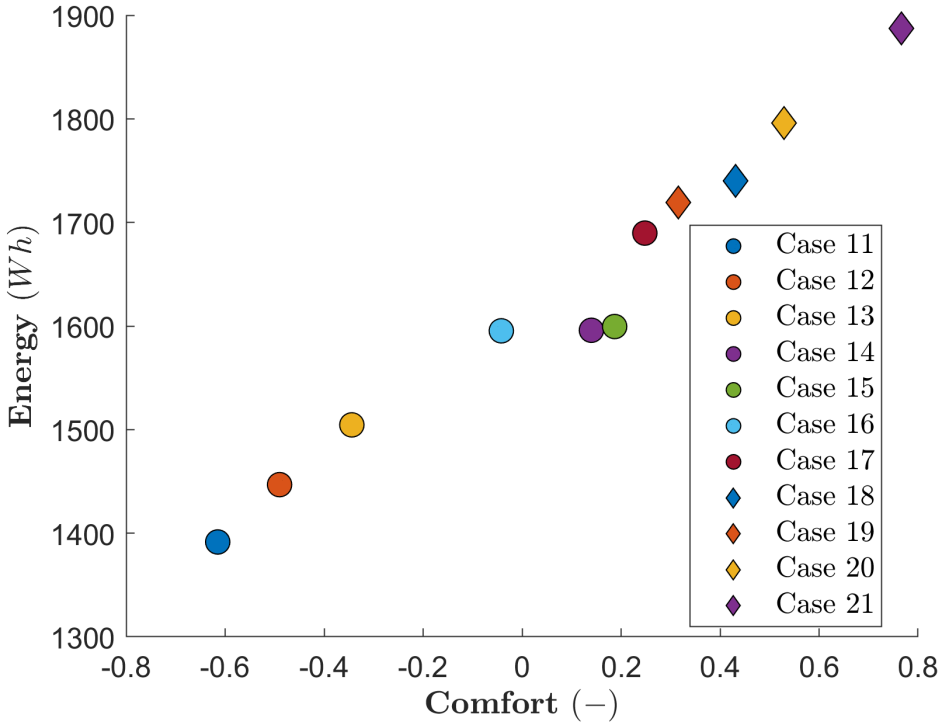

Figure 4.27: Comparison of total energy spent against comfort after 30 minutes of heat-up.

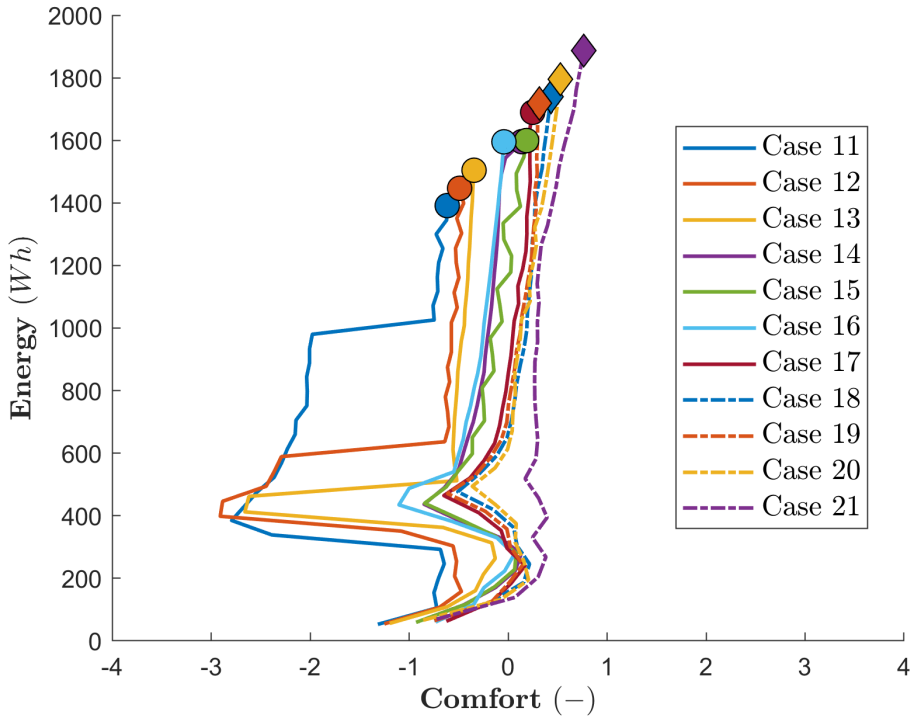

Figure 4.28: Comparison of total energy spent against comfort during the first 30 minutes of heat-up. The line plots the time history of each case.

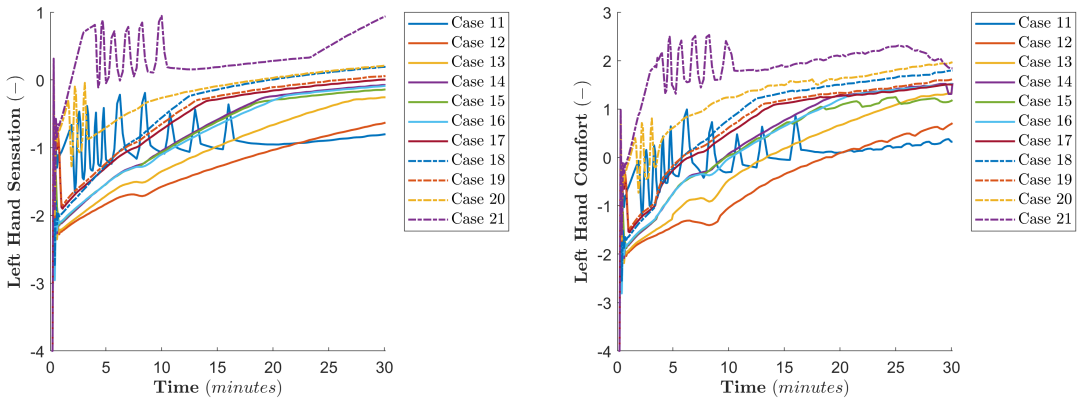

Figure 4.29: Comparison of hand sensation (left fig) and comfort (right fig) against time, using left hand data.

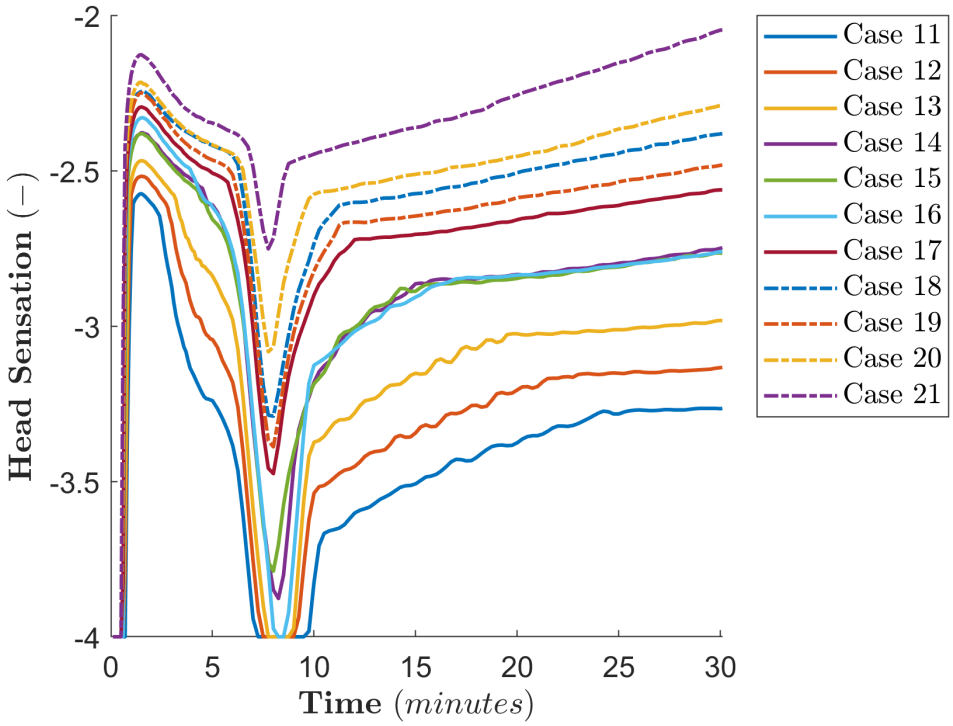

Figure 4.30: Comparison of head sensation against time.

4.3 Energy and comfort evaluation

The TTC for all the cases is summarized in the table 4.7.

Case	HVAC power [W]	Seat/STW temp [°C]	Rad panel temp [°C]	TTC [min]	Energy [Wh]	Comfort fluctuation
Base case 1	2500	N/A	N/A	N/A	1250	N/A
Base case 2	3500	N/A	N/A	12.5	1750	yes
Base case 3	4500	N/A	N/A	2.0	2250	no
Case 1	1300	20	65	N/A	754	N/A
Case 2	1700	25	50	N/A	936	N/A
Case 3	2200	30	45	N/A	1181	N/A
Case 4	2500	35	80	N/A	1385	N/A
Case 5	2600	50	75	N/A	1455	N/A
Case 6	3200	40	55	11.4	1701	yes
Case 7	3800	45	65	1.4	2017	no
Case 8	400	45	60	1.2	2107	no
Case 9	4300	30	70	3.0	2242	no
Case 10	4800	35	40	N/A	2452	N/A
Case 11	2600	35/24.5	50	N/A	1392	N/A
Case 12	2700	25/17.5	65	N/A	1447	N/A
Case 13	2800	15/10.5	80	N/A	1505	N/A

Case	HVAC power [W]	Seat/STW temp [$°C$]	Rad panel temp [$°C$]	TTC [min]	Energy [Wh]	Comfort fluctuation
Case 14	3000	15/10.5	75	N/A	1596	N/A
Case 15	3000	25/17.5	70	N/A	1599	N/A
Case 16	3100	10/7	40	N/A	1595	N/A
Case 17	3200	30/21	60	14.9	1690	yes
Case 18	3300	20/14	70	11.15	1719	yes
Case 19	3300	30/21	45	12.9	1740	yes
Case 20	3400	35/24.5	60	10.15	1796	yes
Case 21	3600	40/28	50	1.8	1887	no

Table 4.7: The table compiles all of the cases, their time to comfort, and energy used in 30 minutes. The last column denotes whether the overall comfort in the given case has crossed the 0 line more than once before TTC.

From the cases that reach comfort the lowest energy usage is 1690 Wh obtained in case 17, where 3200 W are used for air heating, and the maximum thermostat temperature are $30°C$ for the seat, $21°C$ for the steering wheel, and $60°C$ for the radiant surfaces. Compared to the closest reference point, which is base case 2, the energy usage is 3.4% lower and the time to comfort is 19.2% longer. While there is some energy saving it is worth noting that it might be within the margin of error due to the limitations in the model.

Another case that is interesting is case nr 21. In this case the positive comfort is reached very quickly and it is maintained throughout the simulation. Additionally it reaches the highest comfort after 30 minutes. It uses 1887 Wh of energy which is considerably less than other cases with similarly low TTC such as case 7 (2017 Wh), case 8 (2107 Wh) and case 9 (2242 Wh). Compared to base case 3 it has 10% faster TTC and saves 16% energy. Which is a much more certain vote of confidence in favor of using the panels.

4.4 Alternative comfort

In the above results a TAITherm calculation of overall comfort based on Berkeley studies was used. This calculation includes a rule that ¨If the two most uncomfortable body segments have local comfort less than -2.5, the most comfortable segment will not be included, and the overall comfort will be calculated as the average of the three most uncomfortable segments.¨ [9]. Due to that rule in the cases in batch 2 the overall comfort is severely reduced by the low local comfort of head and neck segments which might not be a realistic representation. Therefore for a comparison an alternative comfort formulation was calculated as a simple average of the local comfort of every segment in the body. Alternative comfort is presented in fig. 4.31.

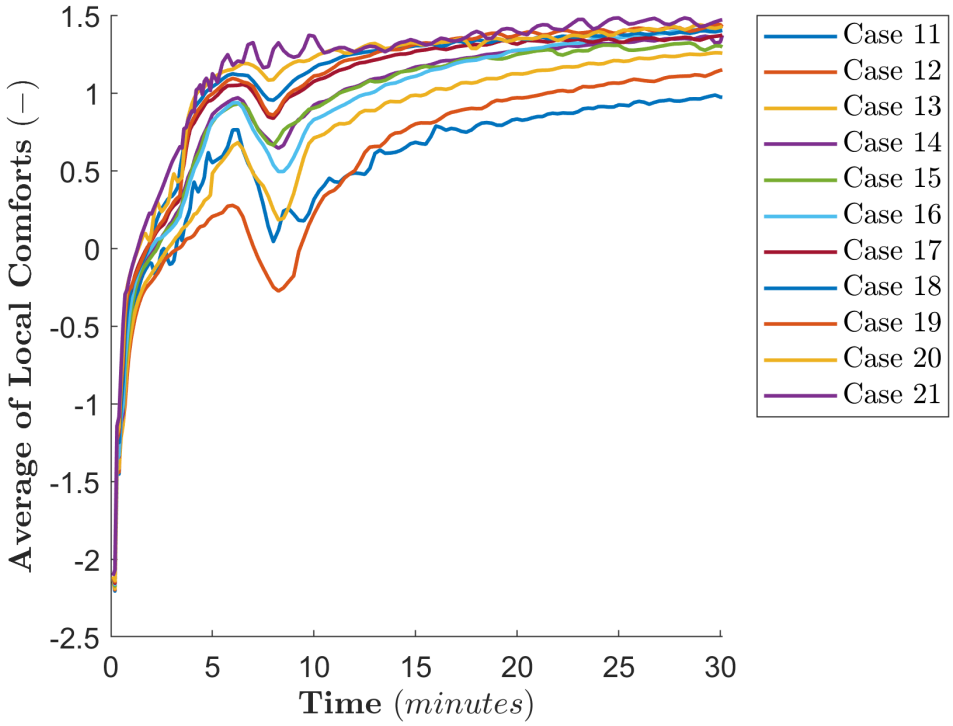

Figure 4.31: Cases 11-21 alternative comfort formulation.

5

Conclusion

The conclusion is that there is a possibility of saving energy by using the panels. For the currently investigated setup of panels a limited amount of savings was achieved, however the panels used very little energy. The case with only panels active showed that, at the highest output setting, the panels still consumed less than a tenth of what the HVAC system consumed. Additionally, in most of the cases the head comfort had a significant impact on the overall comfort. In this work a metric of maintained positive comfort was used and for cases like case 14, 15 and 16 the influence of the head local comfort was significant enough to reduce it below the qualifying threshold. Using the alternative comfort formulation, described in the previous section, those cases would qualify and could provide higher energy saving. Moreover, it is not certain whether the results of local sensation on the head segment are realistic, since the air temperature of the air nodes around it does not exhibit any sudden jumps in temperature. Additionally, since the accuracy of the flow field is limited it can also have an adverse impact on the accuracy of the head segment predictions. The advection links are based on a fully-developed flow field and the same is true for fluid velocities estimations used in calculation of convection on the manikin surfaces. Since the velocity on the head element is higher than the neighbouring parts, it can be more sensitive to the inaccuracies. It would be interesting to validate the model against physical tests as well as other metrics for comfort such as the equivalent temperature approach.

In addition, in author's opinion it would be beneficial to use more heated surfaces to get higher comfort results with lower energy usage. In the current setup the bulk of energy usage is still input into the HVAC system. An investigation into a more balanced setup with a higher share of power directed to the panels could produce more efficient output. Lastly, assuming that the calculation of local comfort on the head segments is correct, adding radiative panels in the roof of the cabin and conductive surface in the headrest would enhance the sensation and comfort of the head and in turn reduce the overall comfort penalty.

5.1 Future work

Due to the limitations and time constraints this work tackles only a small portion of questions regarding the localized heating in a car cabin. More work could be done in terms of the process improvement and further optimization study. This includes but is not limited to:

- Use curves of heat rate to better model the initial phase of the HVAC heating
- Coupling the surface simulation in TAITherm with a transient CFD simulation to achieve better resolution of the flow field.
- Improving on the thermostat script to smooth out the temperature oscillations. For example a PID controller script could be implemented.
- Try different combination of active panels.
- Rerun the simulation using different manikin setup. For example change the male manikin to a female one, change the clothing ensemble, add the passengers.
- Try to analyze efficiency of cabin heating with localized heating and a heat pump based HVAC system.

Bibliography

[1] G. D. Mathur, Vehicle Thermal Management : Heat Exchangers & Climate Control, SAE International, 2004.

[2] F. Nielsen, Automotive Climate Systems: Investigation of Current Energy Use and Future Measures, Goteborg: Chalmers University of Technology, 2016.

[3] M. Jeffers, L. Chaney and J. Rugh, "Climate Control Load Reduction Strategies for Electric Drive Vehicles in Cold Weather," SAE Int. J. Passeng. Cars - Mech. Syst. 9(1), 2016.

[4] C. Chongpyo , K. Gangchul, P. Youngdug and L. Wookhyun , "The development of an energy-efficient heating system for electric vehicles," in 2016 IEEE Transportation Electrification Conference and Expo, Asia-Pacific (ITEC Asia-Pacific) Transportation Electrification Asia-Pacific (ITEC Asia-Pacific), 2016 IEEE Conference and Expo. :883-885, 2016.

[5] R. B. Anandh, "Effect of Cabin Insulation on the Heating Performance in EVs at Low Temperatures," SAE International, 2023.

[6] M. Lorenz, D. Fiala, M. Spinnler and T. Sattelmayer, "A Coupled Numerical Model to Predict Heat Transfer," SAE Technical Paper, no. 0664, 04 01 2014.

[7] ThermoAnalytics, Inc., "User Guide TAITherm Version 2023.2.0," 2023.

[8] D. Fiala, K. J. Lomas and M. Stohrer, "A computer model of human thermoregulation for a wide range of environmental conditions: the passive system," J Appl Physiol, vol. 87, no. 5, pp. 1957-1972, 1999.

[9] ThermoAnalytics, Inc., "Human Modeling User Guide TAITherm Version 2023.2.0," 2023.

[10] H. Zhang, Human thermal sensation and comfort in transient and non-uniform thermal environments (Ph.D. Thesis), University of California, Berkeley, 2003.

[11] H. Zhang, E. Arens, C. Huizenga and T. Han, "Thermal sensation and comfort

models for non-uniform and transient environments: Part I: Local sensation of individual body parts„" Building and Environment, vol. 45, no. 2, pp. 380-388, 2010.

[12] H. Zhang, E. Arens, C. Huizenga and T. Han, "Thermal sensation and comfort models for non-uniform and transient environments, part II: Local comfort of individual body parts," Building and Environment, vol. 45, no. 2, pp. 389-398, 2010.

[13] H. Zhang, E. Arens, C. Huizenga and T. Han, "Thermal sensation and comfort models for non-uniform and transient environments, part III: Whole-body sensation and comfort," Building and Environment, vol. 45, no. 2, pp. 399-410, 2010.

[14] A. R. Tiley, The measure of man and woman: Human factors in design, Hoboken, Nj: John Wiley and Sons, 2002.

[15] F. P. Incropera, Fundamentals of heat and mass transfer (5. ed.), John Wiley and Sons, 2002.

[16] R. Zevenhoven, Introduction to Process Engineering, Åbo Akademi University, 2013.

A

Appendix 1 - Thermostat code

This code is written in JavaScript and it is executed by TAITherm during the simulation. It uses TAITherm API.

```
// Variables to be read from user defined string in Hook
   Functions (Analyze>Params>Hook Functions)
    var dT = 0.5;
    var powerOff = 0;

// Initialize arrays to store T and P values
    var T_values = [];
    var P_values = [];
    var T1 = 0;
    var P1 = 0;
    var T2 = 0;
    var P2 = 0;
    var T3 = 0;
    var P3 = 0;
    var T4 = 0;
    var P4 = 0;
    var T5 = 0;
    var P5 = 0;
    var T6 = 0;
    var P6 = 0;

    var sensorElem1 = 112956; //Seat cushion
    var sensorElem2 = 113235; //seat back
    var sensorElem3 = 194545; //STW
    var sensorElem4 = 145275; //FLT door
    var sensorElem5 = 145903; //FLB door
    var sensorElem6 = 176843; //panel under STW

//Variables to be used in this user routine
    var heaterOn1 = true;
    var heatRate1 = 0;
```

```
    var heaterOn2 = true;
    var heatRate2 = 0;
    var heaterOn3 = true;
    var heatRate3 = 0;
    var heaterOn4 = true;
    var heatRate4 = 0;
    var heaterOn5 = true;
    var heatRate5 = 0;
    var heaterOn6 = true;
    var heatRate6 = 0;

// The solution start hook function initializes any global
   variables needed
// by the other functions.  This allows a single check to be
    performed to
// see if all variables were set propertly.

// If a global variable is not initializes, an error message
    is printed to the
// console window.
function ReadVarSolutionStart( userString )
{
    var api = new API;
    var modelName = new ReturnValueString;
    api.modelFileName(modelName);
    var tdfFile = new File(modelName.value);
    var f = new File(tdfFile.path + "/input.txt");
    f.open(File.ReadOnly);

    while (!f.eof) {
        var line = f.readLine();
        // Split the line by comma to separate temperature
           and pressure
        var values = line.split(',');

        // Parse the values as floats and push them to the
           respective arrays
        T_values.push(parseFloat(values[0]));
        P_values.push(parseFloat(values[1]));
    }

    f.close();
    System.println("Got temp values: " + T_values.join(", ")
       );
    System.println("Got power values: " + P_values.join(",
       "));
```

```
    T1 = T_values[0];
    P1 = P_values[0];
    T2 = T_values[1];
    P2 = P_values[1];
    T3 = T_values[2];
    P3 = P_values[2];
    T4 = T_values[3];
    P4 = P_values[3];
    T5 = T_values[4];
    P5 = P_values[4];
    T6 = T_values[5];
    P6 = P_values[5];

    System.println("Got T1 set : "+(T1));
    System.println("Got P1 set : "+(P1));
    System.println("Got T2 set : "+(T2));
    System.println("Got P2 set : "+(P2));

}


// This is an internal function used to return the sensor
   temperature.  Currently
// this function returns the front temperature of the sensor
    element.
function sensorTemperature1()
{
    var temp = 20;

    // Retrieves the FRONT SURFACE temperature of the
       element
    var api = new API;
    var elemNodeIdx = new ReturnValueInt;
    var sensorElemIdx = new ReturnValueInt;

    var status = api.getElementIndex(sensorElem1,
       sensorElemIdx); // Using sensorElem1
    if (status != api.success) api.abortSolutionWithMessage
       ("Invalid Element ID " + sensorElem1);

    status = api.elementSurfaceNode(sensorElemIdx.value, api
       .front, elemNodeIdx);

    if (status == api.success) {
        var nodeTemp = new ReturnValueDouble;
```

```
        status = api.getTemperature(elemNodeIdx.value,
            nodeTemp);

        if (status == api.success)
            temp = nodeTemp.value - 273.15;
        else
            System.println("Failed to retrieve temperature
                of node " + elemNodeIdx.value);
    } else {
        System.println("Failed to retrieve the temperature
            of element " + sensorElem1);
    }

    return temp;
}

// This hook function is called at the end of the time step
   to see if the fan should be turned
// on or off for the next time step.
function heaterTimeStepEnd1( userString )
{
    //if(heaterOn) System.println("The heater is currently
       ON");
    //else System.println("The heater is currently OFF");

    var sensorTemp1 = 0.0;
    sensorTemp1 = sensorTemperature1();
    System.println("sensor1 temperature  = " + (sensorTemp1)
        + " C");
    if (sensorTemp1 < (T1-dT)) {
        System.println("  Turning heater1 ON" );
        // Turn heater on
        heaterOn1 = true;
    }
    else if (sensorTemp1 > (T1)) {
        System.println(" Turning heater1 OFF" );
        // Turn heater off
        heaterOn1 = false;
    }
    else {
        // Keep the current setting for heater
    }
    System.println(" ");
}
```

```
// This function is used to return the Heat Rate for the for
    the heater.
// This function looks at the flag to see if the heater is
   on or off and returns
// the appropriate heat rate.
function heaterRate1( userString, inputData )
{
    //Adding stuff to get part and element areas
        var inputData = arguments[1];
        var partArea = inputData.partArea;
        var elemArea = inputData.nodeArea;
         //System.println("got Part Area  "+(partArea));
         var powerElement1 = 0.0;
//Adding stuff to get part and element areas

    if (heaterOn1) {
//Adding stuff to get part and element areas
        powerElement1 = P1*(elemArea/partArea);
//Adding stuff to get part and element areas
        return powerElement1;
    }
    else {
        return powerOff;
    }
}

//SECOND PANEL
    ------------------------------------------------------------------------


function sensorTemperature2()
{
    var temp = 20;

    // Retrieves the FRONT SURFACE temperature of the
       element
    var api = new API;
    var elemNodeIdx = new ReturnValueInt;
    var sensorElemIdx = new ReturnValueInt;

    var status = api.getElementIndex(sensorElem2,
       sensorElemIdx); // Using sensorElem2
    if (status != api.success) api.abortSolutionWithMessage
       ("Invalid Element ID " + sensorElem2);

    status = api.elementSurfaceNode(sensorElemIdx.value, api
       .front, elemNodeIdx);
```

```
    if (status == api.success) {
        var nodeTemp = new ReturnValueDouble;
        status = api.getTemperature(elemNodeIdx.value,
           nodeTemp);

        if (status == api.success)
            temp = nodeTemp.value - 273.15;
        else
            System.println("Failed to retrieve temperature
               of node " + elemNodeIdx.value);
    } else {
        System.println("Failed to retrieve the temperature
           of element " + sensorElem2);
    }

    return temp;
}

// This hook function is called at the end of the time step
   to see if the fan should be turned
// on or off for the next time step.
function heaterTimeStepEnd2( userString )
{
    //if(heaterOn) System.println("The heater is currently
       ON");
    //else System.println("The heater is currently OFF");

    var sensorTemp2 = 0.0;
    sensorTemp2 = sensorTemperature2();
    System.println("sensor2 temperature  = " + (sensorTemp2)
        + " C");
    if (sensorTemp2 < (T2-dT)) {
        System.println("  Turning heater2 ON" );
        // Turn heater on
        heaterOn2 = true;
    }
    else if (sensorTemp2 > (T2)) {
        System.println(" Turning heater2 OFF" );
        // Turn heater off
        heaterOn2 = false;
    }
    else {
        // Keep the current setting for heater
    }
    System.println(" ");
```

```
}

// This function is used to return the Heat Rate for the for
    the heater.
// This function looks at the flag to see if the heater is
   on or off and returns
// the appropriate heat rate.
function heaterRate2( userString, inputData )
{
    //Adding stuff to get part and element areas
        var inputData = arguments[1];
        var partArea = inputData.partArea;
        var elemArea = inputData.nodeArea;
         //System.println("got Part Area  "+(partArea));
         var powerElement2 = 0.0;
//Adding stuff to get part and element areas

    if (heaterOn2) {
//Adding stuff to get part and element areas
        powerElement2 = P2*(elemArea/partArea);
//Adding stuff to get part and element areas
        return powerElement2;
    }
    else {
        return powerOff;
    }
}

.
.
.
```

The actual thermostat code goes further but it is omitted in this appendix for brevity. Further part of the code is just repeating the code that was used for the second panel for each subsequent panel with appropriate variables.

DEPARTMENT OF MECHANICS AND MARITIME SCIENCES
CHALMERS UNIVERSITY OF TECHNOLOGY
Gothenburg, Sweden 2024
www.chalmers.se

CHALMERS
UNIVERSITY OF TECHNOLOGY